

NASA TECHNICAL NOTE



NASA TN D-3603

c.1

NASA TN D-3603

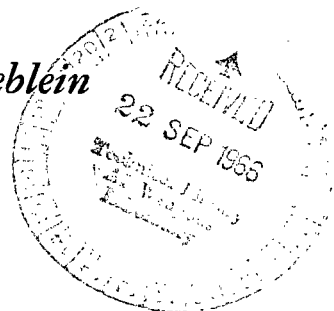


LOAN COPY: RETURN
AFWL (WLIL-2)
KIRTLAND AFB, N M

ANALYSIS AND CORRELATION OF HEAT-TRANSFER COEFFICIENT AND FRICTION FACTOR DATA FOR DILUTE GAS-SOLID SUSPENSIONS

by Robert Pfeffer, Salvatore Rossetti, and Seymour Lieblein

*Lewis Research Center
Cleveland, Ohio*





**ANALYSIS AND CORRELATION OF HEAT-TRANSFER COEFFICIENT AND
FRICTION FACTOR DATA FOR DILUTE GAS-SOLID SUSPENSIONS**

By Robert Pfeffer, Salvatore Rossetti, and Seymour Lieblein

**Lewis Research Center
Cleveland, Ohio**

NATIONAL AERONAUTICS AND SPACE ADMINISTRATION

**For sale by the Clearinghouse for Federal Scientific and Technical Information
Springfield, Virginia 22151 - Price \$2.50**

CONTENTS

	Page
SUMMARY	1
INTRODUCTION	2
THERMOPHYSICAL PROPERTIES	3
Bulk Density	3
Specific Heat	4
Thermal Conductivity	4
Viscosity	6
Specific Heat Ratio	7
Sonic Velocity	9
CONVECTIVE HEAT TRANSFER	10
Data Sources	11
Farbar and Morley	12
Farbar and Depew	13
Danziger	13
Schluderberg, Whitelaw, and Carlson	14
Franklin Institute	15
Gorbis and Bakhtiozin	16
Tien	18
Tien and Quan	19
Mickley and Trilling	19
List	20
Correlations	20
Effect of loading ratio and specific heat ratio	20
Effect of particle diameter	23
Effect of gas Reynolds number	25
Final form of correlation	26
PRESSURE DROP	28
Pure Gas Relations	28
Flow Regimes	29
Analytical Models	29
Drag coefficient model	30
Equivalent friction factor model	32
Reynolds analogy	33

Eddy viscosity model	35
Data Sources	36
Peskin and Dwyer.	37
Peskin.	37
Mehta, Smith, and Comings	38
Farbar	40
Dogin and Lebedev	40
Vogt and White	41
Other work	42
Correlations	43
Equivalent friction factor based on eddy viscosity model	43
Equivalent friction factor by use of Reynolds analogy.	44
Comparison of models with experimental data	47
Effect of particle diameter	48
Final correlations	49
APPLICATION OF RESULTS	49
SUMMARY OF RESULTS	51
APPENDIX - SYMBOLS.	52
REFERENCES.	55

ANALYSIS AND CORRELATION OF HEAT-TRANSFER
COEFFICIENT AND FRICTION FACTOR DATA
FOR DILUTE GAS-SOLID SUSPENSIONS

by Robert Pfeffer, * Salvatore Rossetti, † and Seymour Lieblein
Lewis Research Center

SUMMARY

The available literature on both the heat transfer and the pressure drop associated with the flow of a dilute gas-solid suspension was reviewed and analyzed. This study obtained workable correlations for predicting some of the basic thermophysical properties and both the heat-transfer coefficient and the friction factor for the flow of suspensions in tubes. The basic properties of suspensions investigated included bulk density, specific heat, thermal conductivity, viscosity, specific heat ratio, and sonic velocity. The variables considered included the loading ratio (pounds of solid per pound of gas), the ratio of particle to gas specific heat, the gas Reynolds number, and the particle diameter.

Two possible correlations for the convective heat-transfer coefficient of a suspension resulted from this analysis. Both correlations indicated that the ratio of suspension to pure gas heat-transfer coefficient increased with loading ratio and specific heat ratio, decreased with increasing gas Reynolds number, and was essentially unaffected by particle diameter for the range of conditions considered.

*Professor of Chemical Engineering, City College of the City University of New York.

†Graduate Student, City College of the City University of New York.

The Reynolds analogy was applied to these heat-transfer relations, and a correlation for the ratio of suspension to gas equivalent friction factor was obtained. The ratio of the suspension friction factor to the pure gas friction factor was found to increase with loading ratio and decrease with gas Reynolds number and to be essentially unaffected by particle diameter. This correlation was found to be in good agreement with both the experimental data and an analytical study based on an eddy viscosity model for a suspension.

INTRODUCTION

Space power generation systems must be capable of continuously generating power for long periods of time. One power generating system currently under consideration is the indirect-conversion closed-loop heat engine. In this system heat is generated in a nuclear or solar source and rejected by a radiator, with power obtained from a turbine. However, because of mission limitations the powerplant specific weight must be kept low.

The Brayton cycle using a pure inert gas as the working fluid has been considered as a potential source of space power (refs. 1, 2, and 3). The basic technology available from developments in the gas turbine and power production fields can be advantageously utilized in Brayton cycle space power applications. However, because of the low temperature levels in the radiator the Brayton cycle waste heat rejection unit becomes very large especially when a gas radiator is used in the power loop. It is apparent, therefore, that if the area and weight of the radiator could be reduced, this system would become more promising for future space missions.

In one approach to circumvent the effects of the inherently low heat-transfer coefficients in radiator gas flow, a second loop containing a liquid-flow radiator in conjunction with a gas-to-liquid heat exchanger and circulating pump can be used instead of the gas flow radiator. However, such an arrangement involves increased complexity and an additional power drain. Another method of decreasing the radiator area, and hence its weight, is to increase the heat-transfer coefficient of the gas working fluid to allow a greater heat transfer per unit of radiation area. Recent studies have shown that the addition of solid particles to a turbulently flowing gas will increase the rate of heat transfer between the gas and its surroundings (refs. 4 to 6). This increase in heat-transfer rate results from two separate effects: an increase in the volumetric heat capacity of the working fluid (because the axial temperature difference is decreased), and an increase in the gas side heat-transfer coefficient. Because of these desirable properties, the use of a gas-solid suspension of small particles is being considered as a coolant for nuclear reactors, and might also be useful as a working fluid in a Brayton cycle space power generating system.

In these applications of dilute flowing gas-solid suspensions, it is necessary to be able to predict the suspension heat-transfer coefficient and pressure drop so that the heat

rejection and pumping equipment can be adequately designed. However, readily usable correlations for predicting both heat-transfer rates and pressure drop of flowing suspensions are not available. In an attempt to establish such correlations, a review and analysis of available experimental data, correlations, and theory pertaining to heat-transfer coefficients and pressure drops of gas-solid suspensions was undertaken. Some of the related thermodynamic and transport properties of gas-solid suspensions were also reviewed. The analysis was limited to dilute suspensions of small particles (loading ratios less than 10 and particle diameters less than 150μ) since these are of primary interest in application to the Brayton cycle.

THERMOPHYSICAL PROPERTIES

The performance of a flowing dilute gas-solid suspension (heat transfer, pressure drop, etc.) will be dependent on the fundamental thermophysical properties of the suspension. In general, these properties of the suspension will be different from those of the pure carrier gas. Thus, before proceeding with the analysis of heat-transfer and pressure drop characteristics, it is necessary to define the principal thermophysical properties of the suspension. Some of the more fundamental thermodynamic and transport properties of interest in a gas-solid suspension are density, specific heat, thermal conductivity, viscosity, specific heat ratio, and sonic velocity. In many cases, the properties of the suspension will be related to those of the pure gas and will invariably be a function of the loading ratio, defined as the ratio of the mass flow rate of solid to the mass flow rate of the pure gas.

Bulk Density

The bulk density of the suspension ρ_s and the densities of the pure substances (particles and gas) are related to the loading ratio η by the equation

$$\frac{\rho_s}{\rho_g} = \frac{\eta + 1}{\eta(\rho_g/\rho_p) + 1} \quad (1a)$$

where

$$\eta = \frac{W_p}{W_g} \quad (1b)$$

Since ρ_g/ρ_p is generally small ($\rho_g/\rho_p < 10^{-3}$) and if $\eta \leq 10$, then $\eta(\rho_g/\rho_p) \ll 1$, and equation (1a) reduces to

$$\frac{\rho_s}{\rho_g} \approx 1 + \eta \quad (1c)$$

(Symbols are defined in the appendix.)

Specific Heat

If a weighted average for the specific heat of the suspension is assumed,

$$\frac{(C_p)_s}{(C_p)_g} = \frac{1 + \eta \left[\frac{(C_p)_p}{(C_p)_g} \right]}{1 + \eta}$$

Since by definition

$$\delta \equiv \frac{(C_p)_p}{(C_p)_g} \quad (2)$$

Then

$$\frac{(C_p)_s}{(C_p)_g} = \frac{1 + \delta\eta}{1 + \eta} \quad (3)$$

A plot of $(C_p)_s/(C_p)_g$ against η for a suspension of graphite particles in helium, neon, and argon is given in figure 1. At large values of η , the heat capacity ratio $(C_p)_s/(C_p)_g$ asymptotically approaches the value of δ for each suspension.

Thermal Conductivity

Gorring and Churchill (ref. 7) have presented an analytical equation that agrees quite well with experimentally measured thermal conductivities of dispersions. They have

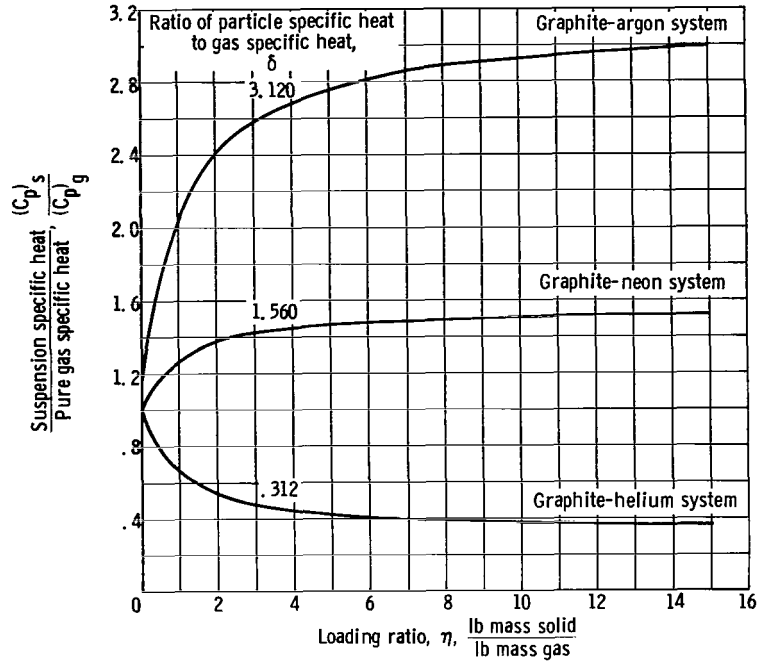


Figure 1. - Effect of loading ratio on ratio of specific heat of suspension to specific heat of pure gas for systems of graphite suspended in helium, neon, and argon. Graphite specific heat, 0.386 Btu/(lb)(°F).

shown that for $\eta < 20$ the effective thermal conductivity of a suspension is given by

$$\frac{k_s}{k_g} = \frac{\beta - \epsilon}{\beta + \epsilon} \quad (4)$$

where ϵ is the fractional solid volume (ft³ solid/ft³ suspension) given by

$$\epsilon = \frac{\eta \rho_g}{\rho_p + \eta \rho_g} = \frac{\eta}{\rho_p / \rho_g + \eta} \quad (5)$$

and

$$\beta = \frac{1 + \frac{k_p}{k_g}}{1 - \frac{k_p}{k_g}}$$

Hence

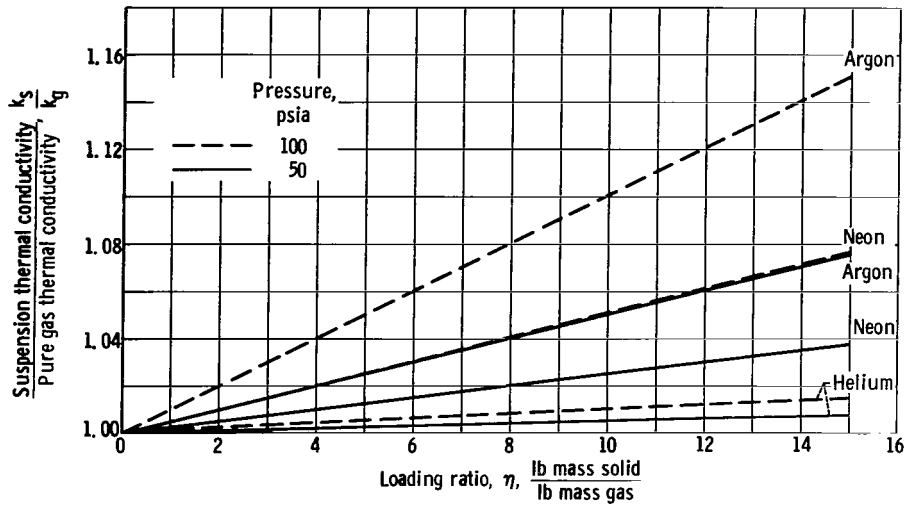


Figure 2. - Effect of loading ratio on ratio of thermal conductivity of suspension to thermal conductivity of pure gas for systems of graphite suspended in argon, neon, and helium. Temperature, 700° R; density of graphite, 105 pounds per cubic foot; thermal conductivity of graphite, 100 Btu/(hr)(ft)(°R).

$$\frac{k_s}{k_g} = \frac{1 + \frac{k_p}{k_g} - \frac{\eta}{\rho_p/\rho_g + \eta} \left(1 - \frac{k_p}{k_g}\right)}{1 + \frac{k_p}{k_g} + \frac{\eta}{\rho_p/\rho_g + \eta} \left(1 - \frac{k_p}{k_g}\right)} \quad (6)$$

Results of sample calculations for k_s/k_g for several gases with graphite particles are shown in figure 2. For $\eta \leq 10$, the conductivity of the suspension was not seen to be very different from that of the pure gas for the cases considered.

Viscosity

Very little experimental or analytical work has been done in determining the viscosity of a gas-solid suspension. The only reference found for experimental work on the viscosity of gas-solid suspensions was done by Sproull (ref. 8) at low loading ratios ($\eta < 1$) with dusty air. The results that Sproull found at these low loading ratios indicate that the viscosity of a gas-solid suspension is actually lower than that of a pure gas; however, at these very low particle concentrations the concept of the viscosity of a suspension becomes nebulous.

In an analytical study Happel (ref. 9), by omitting the inertia terms in the steady-state Navier-Stokes equations, derived the following relation between relative viscosity and solid concentration that is in good agreement with existing data at high loading ratios ($\eta > 20$):

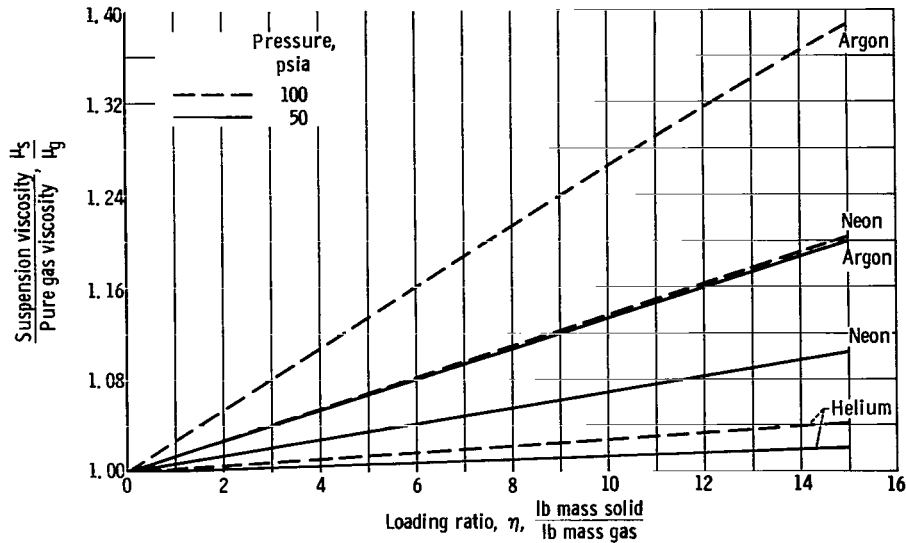


Figure 3. - Effect of loading ratio on ratio of viscosity of suspension to viscosity of pure gas for systems of graphite suspended in argon, neon, and helium. Temperature, 700° R; density of graphite, 105 pounds per cubic foot.

$$\frac{\mu_s}{\mu_g} = 1 + 5.5 \epsilon \psi \quad (7a)$$

where ϵ is the fraction of volume occupied by solids as given by equation (5), and ψ is a factor characteristic of the loading ratio.

For $\eta < 10$, $\psi \rightarrow 1.0$, and equation (7a) reduces to

$$\frac{\mu_s}{\mu_g} = 1 + 5.5 \epsilon \quad (7b)$$

which is identical in form to the Einstein equation (ref. 10), except for the difference in the constant, 5.5 for equation (7b) as compared with 2.5 for the Einstein equation. Sample results for μ_s/μ_g , as given by equation (7b), are shown in figure 3 for three gases with graphite particles. As can be seen in the figure, the suspension viscosity may be substantially different from the gas viscosity for heavy gases at high pressure.

Specific Heat Ratio

The effective isentropic specific heat ratio γ_s for a suspension can be readily obtained from an energy balance if the temperature and velocity of the particles in the suspension are assumed to be the same as the temperature and velocity of the gas (refs. 11 and 12). Based on these assumptions and using the ratio of the specific heat of the particles to the specific heat of the gas δ , the ratio of specific heat ratios in terms of the loading ratio η becomes

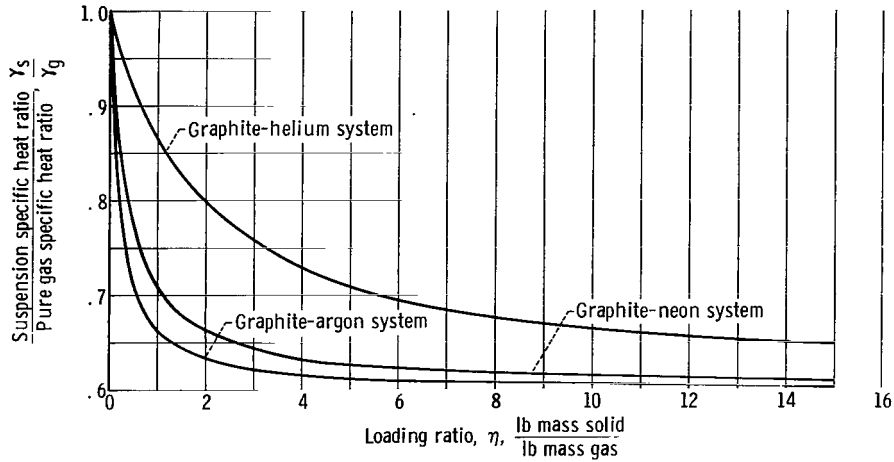


Figure 4. - Effect of loading ratio on ratio of specific heat ratios for various gas-solid suspensions.

$$\frac{\gamma_s}{\gamma_g} = \frac{1 + \delta\eta}{1 + \gamma_g \delta\eta} \quad (8)$$

For large loading ratios, $\eta > 10$, $\gamma_s \rightarrow 1.0$, and the suspension behavior approaches that of an incompressible fluid. Figure 4 is a plot of the ratio of the isentropic specific heat ratios γ_s/γ_g as a function of η for suspensions of graphite particles in inert gases. The figure indicates that for neon and argon γ_s/γ_g decreases rapidly as η increases. For the graphite-helium system, the decline in γ_s/γ_g with η is less pronounced because of the low value of δ for this system. For all three systems γ_s/γ_g approaches the asymptotic value of 0.6.

Since solid particles can do no expansion work, their presence in components involving flow expansion, such as rocket nozzles or gas turbines, can only decrease the effectiveness of the expansion process in converting thermal energy to kinetic energy. The particles are accelerated entirely by drag forces associated with lag or slippage of the particles relative to the expanding gas; therefore, some performance loss relative to the calculated ideal no-slip expansion must be present when dealing with solid particles. Experience has shown that both velocity lag and thermal lag become significant as the size of the particles and the particle loading ratio increase; therefore, the value of γ_s given by equation (8) is at best an approximation or a limiting value.

A simplified one-dimensional analysis by Kleigel (ref. 13) for a gas-solid suspension flow in a rocket nozzle shows that γ_s increased from the equilibrium value given by equation (8) as the particle was accelerated but was rather insensitive to particle lag for small lags. This analysis indicates that the use of equation (8) to estimate γ_s may be a reasonable approximation even for nonequilibrium flow when the particle size is small. In a nozzle expansion, for example, 1- to 2-micron particles were found to follow the gas

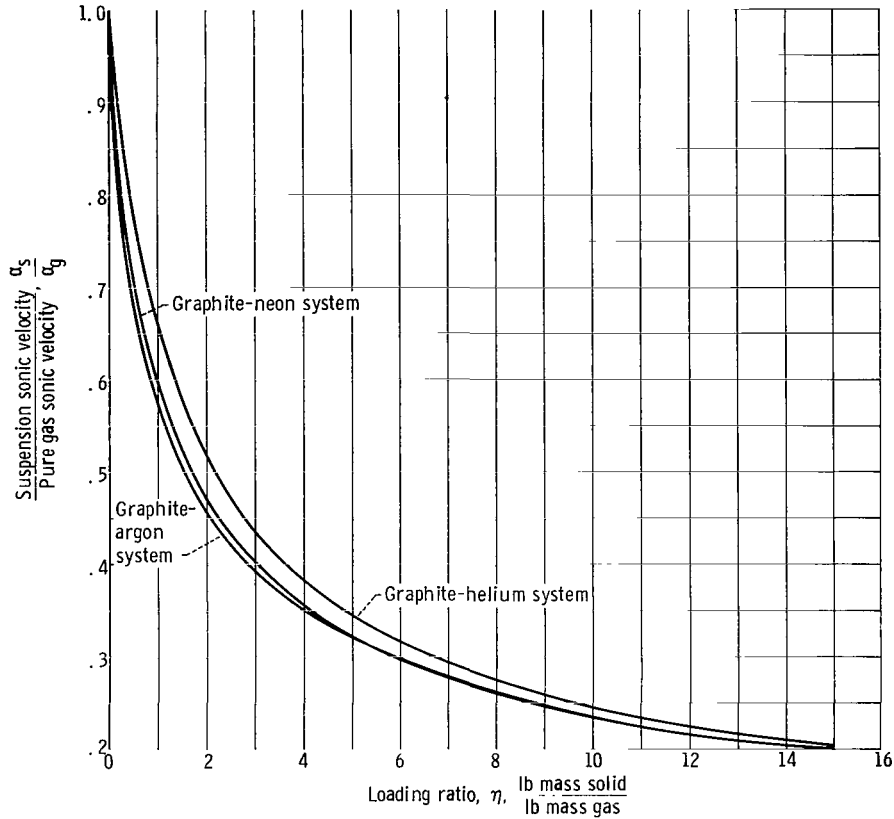


Figure 5. - Effect of loading ratio on ratio of suspension sonic velocity to gas sonic velocity.

closely, whereas 10-micron particles had a significant lag (ref. 13) in the throat of the nozzle.

Sonic Velocity

Assuming that $V_p = V_g$ and $T_p = T_g$ gives the velocity of sound in the suspension as (ref. 12)

$$\frac{\alpha_s}{\alpha_g} = \left(\frac{\gamma_s/\gamma_g}{1 + \eta} \right)^{1/2} \quad (9)$$

where α_g is the velocity of sound in the pure gas at the same temperature. Equation (9) shows that the sonic speed of the suspension α_s is always less than that of a pure gas. A plot of α_s/α_g against η is given in figure 5. The figure shows that the sonic velocity of the suspension, as given by equation (9), decreases rapidly as η is increased;

however, how this variation will affect the compressibility and choking of the flow of a dilute suspension in which only the gas carrier is essentially the compressible phase is not clear.

CONVECTIVE HEAT TRANSFER

There appear to be two possible mechanisms explaining why the addition of solid particles to a turbulently flowing gas will increase the rate of heat transfer between the gas and its surroundings. In the first mechanism this increase in heat-transfer rate is attributed to the particles eroding away some of the stagnant gas film at the containing surface and thereby reducing the resistance to heat transfer between the particles and the surface. In the other suggested mechanism the heat transfer from the particles to a surface is mainly affected by the mechanical contact with the wall of particles or groups of particles that are continuously replaced at the exchanger surface. In this model, particles at the bulk temperature of the suspension are swept to the heat-transfer surface by the turbulent motion of the suspension. Here, the relatively high temperature gradient between the heat-transfer surface and the particle adjacent to it transfers heat by conduction at the surface-particle contact. As the temperature of the particle begins to approach that of the heat-transfer surface, the driving potential is reduced and heat flows less rapidly. Thus, achievement of a large heat-transfer coefficient is dependent on vigorous agitation within the bulk of the suspension and on short residence times for the particle at the heat-transfer surface.

If the increased heat transfer is due only to the mechanical shear of the laminar gas film by the particles, the coefficient might appear to depend on the loading ratio but should be independent of the specific heat and thermal conductivity of the solid. On the other hand, if the increase in heat-transfer rate is due to contact of particles with the wall surface, then it would be expected that the thermal conductivities of the solid and gas play a significant role in determining the heat-transfer coefficient. Further experimental studies on a number of dissimilar solids and gases might elucidate the true mechanism of the action of the solids.

Since there is no general agreement on the mechanism by which heat-transfer coefficients of gases are increased by the addition of solids, no attempt will be made to validate either concept. Rather, it will be the purpose of this section to review the analytical and experimental literature dealing with heat-transfer coefficients of gas-solid suspensions in order to obtain a working correlation for the ratio of the heat-transfer coefficient of the suspension to the heat-transfer coefficient of the pure gas h_s/h_g for fully developed turbulent flow in circular tubes.

The ratio of suspension to pure gas heat-transfer coefficient can be obtained by

relating the measured coefficient at various loading ratios to the measured coefficient at $\eta = 0$ or by relating the suspension Nusselt number to the pure gas Nusselt number. The Nusselt number of the suspension is defined as

$$\text{Nu}_s = \frac{h_s D}{k_s} \quad (10)$$

For the pure gas (ref. 14)

$$\text{Nu}_g = \frac{h_g D}{k_g} = 0.023 \text{Re}_g^{0.8} \text{Pr}_g^{0.3} \quad \text{for cooling} \quad (11)$$

and

$$\text{Nu}_g = \frac{h_g D}{k_g} = 0.023 \text{Re}_g^{0.8} \text{Pr}_g^{0.4} \quad \text{for heating} \quad (12)$$

In terms of Nusselt numbers

$$\frac{h_s}{h_g} = \frac{\text{Nu}_s k_s}{\text{Nu}_g k_g} \quad (13a)$$

However, for the test conditions of the available experimental data and correlations, k_s/k_g , as computed by equation (6), was generally sufficiently close to unity (<1.05) for $\eta \leq 10$ so that for simplicity

$$\frac{h_s}{h_g} \cong \frac{\text{Nu}_s}{\text{Nu}_g} \quad (13b)$$

Note in equation (13b) that the Nusselt number ratio should be evaluated for the same gas conditions for which the heat-transfer coefficient ratio is desired (e.g., same gas pressure, temperature, and volumetric flow rate for the suspension and pure gas flows).

Data Sources

Many experimental studies have attempted to investigate the effect of different

TABLE I. - SUMMARY OF OPERATING CONDITIONS UTILIZED IN HEAT-TRANSFER WORK CITED

Particle	Gas	Specific heat ratio, δ	Particle diameter, D_p , μ	Loading ratio, η	Gas velocity, V_g , ft/sec	Tube inside diameter, D , in.	Gas Reynolds number, Re_g	Ratio of tube length to tube diameter, L/D	Test condition	Fluid temperature, T , $^{\circ}F$	Source
Silica-alumina catalyst	Air	^a 1.15	10 to 210 (50 μ avg)	0 to 13.3	38.5 to 81	0.7	13 000 to 28 000	46.6	Heating	75 to 102	Farbar and Morley (ref. 4)
Glass	Air	0.797	30, 70, 140, 200	0 to 10.5	41 to 71	0.67	15 300 to 26 500	47	Heating	-----	Farbar and Depew (ref. 15)
Silica-alumina catalyst	Air	0.84	10 to 210 (50 μ avg)	2 to 446	1.4 to 61.5	0.688 to 1.5	178 to 25 400	240	Cooling	1050	Danziger (ref. 5)
Graphite	Nitrogen, helium, carbon tetra-fluoride, carbon dioxide	0.315 to 1.50	1 to 5	0 to 90	20 to 200	0.313 to 0.875	2000 to 400 000	100 to 289	Heating	90 to 1100	Schluderberg, Whitelaw and Carlson (ref. 18), and Franklin Inst. (ref. 19)
Graphite	Air	0.84 to 1.03	150, 1440, 400, 770, 1160, 2080	0 to 32	25 to 95	0.473 to 1.3	7000 to 65 000	50	Heating	-----	Gorbis and Bakhtiozin (ref. 6)
Glass and lead	Air	0.80 to 0.133	30, 200	0 to 3	40 to 85	0.71	15 000 to 30 000	46.4	Heating	100	Tien and Quan (ref. 23)
Glass	Air	0.80	40, 284, 100, 450, 150, 270	45 to 1600	0.8 to 15	1 to 4	225 to 16 800	Fluidized bed	Heating	120 to 230	Mickley and Trilling (ref. 24)
Glass and copper	Air	0.80, 0.675	50, 534, 224, 586, 392, 356	0.1 to 16.5	10 to 34	$1\frac{1}{2}$ to 2	7250 to 33 000	60 to 80	Heating	85 to 350	List (ref. 25)

^aThis value has been disputed by Danziger (ref. 5).

physical parameters on the heat-transfer coefficient of gas-solid suspensions. A brief summary of the more important and up-to-date research that has been done in this field will now be presented. For convenience, a summary of the principal operating conditions and physical properties used by each investigator appears in table I.

Farbar and Morley. - An exploratory paper by Farbar and Morley (ref. 4) studied the effect on heat-transfer rate of adding silica-alumina catalyst particles to air flowing in a tube 0.7 inch in diameter. The particle size D_p was not uniform but varied from 10 to 210 microns with half of the particles smaller than 50 microns. The range of gas Reynolds number Re_g varied between 13 000 and 28 000, and the loading ratio η was varied between 0 and 13.3. Farbar and Morley found that for a solid loading ratio of unity or less there is practically no effect on the value of the heat-transfer coefficient,

whereas at η greater than 1, the heat-transfer coefficient increased as η was increased. They also found that increasing the gas Reynolds number had a smaller effect on the heat-transfer coefficient of the suspension than on that for a pure gas. This is revealed in their final correlation, which is given by

$$\text{Nu}_s = 0.14 \text{Re}_g^{0.6} \eta^{0.45} \quad (14)$$

If equation (14) is divided by equation (12) and the Prandtl number for air is taken as 0.75, the heat-transfer coefficient ratio becomes

$$\frac{h_s}{h_g} = 6.8 \text{Re}_g^{-0.2} \eta^{0.45} \quad (15)$$

The ratio of specific heats δ and the particle diameter D_p do not appear in their correlation since all of Farbar and Morley's experiments were run with only one gas and one suspension material.

Farbar and Depew. - In a paper by Farbar and Depew (ref. 15), the work of Farbar and Morley was extended in order to attempt to isolate and determine the effect of particle diameter on the heat transfer of gas-solid suspensions. In this study spherical glass particles of four uniform sizes (30, 70, 140, and 200 μ) were added to air flowing vertically in a borosilicate glass tube. The loading ratio was varied from 0 to 10, while the gas Reynolds number was held constant at 15 300, 19 700, and 26 500. The results indicated a substantial increase in the gas-side heat-transfer coefficient for the 30-micron particles, a moderate increase for the 70-micron particles, a slight increase for the 140-micron particles, and essentially no increase for the 200-micron particles for the range of variables covered. The results of Farbar and Depew were not correlated although they did clearly indicate a decrease in heat-transfer coefficient with increase in particle diameter. The data also indicated a decrease in h_s/h_g with increasing gas Reynolds number at a given loading ratio and particle size.

Danziger. - W. J. Danziger (ref. 5) presented a report in which a correlation of the heat-transfer coefficients of silica-alumina cracking catalyst of about 50-micron average particle size in vertical transport was obtained. His data were obtained on recycle catalyst coolers of two designs, both used vertical, single-tube pass, removable-bundle, fire-tube boilers with air-catalyst mixture flowing upward through the tubes. The correlation that Danziger obtained based on two sets of data, his own data for cooling and the data of Farbar and Morley for heating is

$$\frac{h_s D}{k_g} = 0.0784 \text{Re}_g^{0.66} \eta^{0.45} \quad (16)$$

Converting this correlation to h_s/h_g by dividing by equation (11) and taking $\text{Pr}_g = 0.75$ gives

$$\frac{h_s}{h_g} = 3.7 \text{Re}_g^{-0.14} \eta^{0.45} \quad (17)$$

This correlation covers gas Reynolds numbers from 178 to 25 400, loading ratios of 2 to 446, and tube inside diameters from 0.689 to 1.497 inches. The correlation is based on both commercial data as well as the laboratory data of Farbar and Morley; however, it is limited to one average particle diameter (50μ) and one value of δ .

Schluderberg, Whitelaw, and Carlson. - In an effort to study the properties of gaseous suspensions as reactor coolants, an extensive research program was conducted that is fully described by a series of reports (e.g., refs. 16 and 17) and is summarized in a paper by Schluderberg, Whitelaw, and Carlson (ref. 18). These studies of heat-transfer and pressure drop of suspensions of 1- to 5-micron graphite particles in carbon dioxide, helium, nitrogen, and carbon tetrafluoride were carried out at gas pressures between 30 and 130 pounds per square inch gage, gas temperatures between 90° and 1100° F, and suspension densities of up to 8 pounds per cubic foot (η up to 90).

The heat-transfer data of references 16 to 18 for tube inside diameters from 0.313 to 0.875 inch and gas Reynolds numbers from 2×10^3 to 4×10^5 were correlated by the following equation:

$$\text{Nu}_s = 0.02 \text{Re}_g^{0.8} \text{Pr}_g^{0.8} (1 + \delta\eta)^{0.45} \quad (18)$$

Therefore, by dividing equation (18) by equation (12), the ratio of the heat-transfer coefficient of the suspension to the heat-transfer coefficient of the pure gas (assuming an average Pr_g of 0.75) can be approximated by

$$\frac{h_s}{h_g} = 0.78 (1 + \delta\eta)^{0.45} \quad (19)$$

Equation (19) indicates that the increase in heat-transfer coefficient ratio depends primarily on the specific heat parameter δ and the loading ratio η . It shows no effect of

gas Reynolds number or particle size on the heat-transfer coefficient ratio.

Franklin Institute. - The Franklin Institute (ref. 19) conducted a critical evaluation of the work reported earlier by Schluderberg, et al. by starting with the original raw data and recalculating all of the heat-transfer coefficients and other correlation parameters. They found that the data, although believed generally unreliable because of faulty heat balances, could be correlated by any of the following equations:

$$\text{Nu}_s = 0.0205 (1 + \eta)^{-0.4} \text{Re}_s^{0.8} \left(\frac{T_s}{T_m} \right)^{0.8} \text{Pr}_s^{0.4} \quad (20)$$

$$\text{Nu}_s = 0.4 \text{Re}_g^{0.5} \text{Pr}_g^{0.5} (1 + \delta\eta)^{0.45} \quad (21)$$

$$\text{Nu}_s = (\text{Re}_s \text{Pr}_s)^{0.42} \quad (22)$$

$$\text{Nu}_s = 0.023 (1 + \eta)^{-0.7} \text{Re}_s^{0.8} \text{Pr}_s^{0.4} \quad (23)$$

and

$$\text{Nu}_s = 0.015 (1 + \eta)^{-0.4} \text{Re}_s^{0.8} \text{Pr}_s^{0.4} \quad (24)$$

where T_s is the bulk temperature of the suspension in $^{\circ}\text{R}$ and T_m is the mean temperature of the wall and the suspension in $^{\circ}\text{R}$,

$$\text{Re}_s = \frac{DV_s \rho_s}{\mu_g} = (1 + \eta) \text{Re}_g$$

and

$$\text{Pr}_s = \frac{(C_p)_s \mu_g}{k_g} = \frac{1 + \delta\eta}{1 + \eta} \text{Pr}_g$$

If equation (21) is divided by Nu_g (eq. (12)) and Pr_g is taken as 0.75, then

$$\frac{h_s}{h_g} = 16.9 \text{Re}_g^{-0.3} (1 + \delta\eta)^{0.45} \quad (25)$$

Equation (25) is similar to Schluderberg's equation (19) except that it also includes a Reynolds number effect; for example, for an average Re_g of about 25 000, the factor $16.9 Re^{-0.3} \approx 0.81$, and equation (25) approaches equation (19).

The other equations are all based on using the physical properties of the suspension in standard pure-fluid heat-transfer correlations, although no attempt was made to include suspension thermal conductivity and viscosity, and therefore offer no apparent advantages. Closer examination reveals that all the equations except equation (23) can be reduced to the same form for h_s/h_g as that in equation (25).

Gorbis and Bakhtiozin. - The heat-transfer characteristics of a gaseous suspension of graphite particles in vertical flow have also been studied by Gorbis and Bakhtiozin (ref. 6). These authors applied the Reynolds analogy to both the gas and solid phases of the gas-solid suspension and then superimposed the results to obtain an approximate expression for the suspension heat-transfer coefficient. For the gas phase, the Reynolds analogy requires that

$$\frac{h_g}{\rho_g (C_p)_g V_g} = \frac{f_g}{2} \quad (26)$$

Similarly, by definition

$$\frac{h_p}{\rho_g (C_p)_p V_p} = \frac{f_p}{2} \quad (27)$$

where f_g and f_p are the Fanning friction factors due to the gas and particles, respectively. The appearance of ρ_g rather than ρ_p in the Reynolds analogy for the solid phase is due to Gorbis and Bakhtiozin's definition of f_p , which is based on the gas-phase density and is defined by the equation

$$f_p = \frac{\Delta P_p}{2\rho_g} \frac{D}{L} \frac{g_c}{V_p^2} \quad (28)$$

where ΔP_p is the additional pressure drop caused by adding particles to the gas stream.

The summation of equations (26) and (27) with the assumption of no slip between the solids and the gas ($V_g = V_p$) yields

$$h_g + h_p = h_s = \frac{1}{2} V_g \rho_g (C_p)_g f_g \left[\frac{(C_p)_p f_p}{(C_p)_g f_g} + 1 \right] \quad (29)$$

so that, from equations (2) and (26),

$$\frac{h_s}{h_g} = 1 + \delta \left(\frac{f_p}{f_g} \right) \quad (30)$$

For the suspension by definition

$$\Delta P_s = 2f'_s \rho_g \frac{L}{D} \frac{V_s^2}{g_c} \quad (31a)$$

and

$$f'_s = f_g + f_p \quad (31b)$$

Thus,

$$\Delta P_g = 2f_g \frac{L}{D} \rho_g \frac{V_g^2}{g_c} \quad (31c)$$

$$\frac{\Delta P_s}{\Delta P_g} = \frac{f'_s}{f_g} = 1 + \frac{f_p}{f_g} \quad (31d)$$

The pressure drop ratio can be related to the loading ratio η by the simple relation Gasterstadt (ref. 20) proposed as far back as 1924:

$$\frac{\Delta P_s}{\Delta P_g} = 1 + F\eta \quad (32)$$

where F is not a constant but a complicated function of gas Reynolds number, particle size, etc. Combining equations (30), (31d), and (32) then gives

$$\frac{h_s}{h_g} = 1 + F\delta\eta \quad (33)$$

Gorbis correlated his experimental data in the form suggested by equation (33)

assuming F to be a function of two dimensionless groups: the gas Reynolds number Re_g and the particle Reynolds number Re_p , where $Re_p = D_p V_{ps} \rho_g / \mu_g$ and V_{ps} is the terminal settling velocity of the particle. The terminal settling velocity is defined as the velocity of the particle for which the drag forces are exactly balanced by the gravitational forces and can be calculated from standard drag-coefficient correlations (e. g., ref. 21). His final correlation is

$$\frac{h_s}{h_g} = 1 + \left(6.3 Re_g^{-0.3} Re_p^{-0.33} \right) \delta \eta \quad (34)$$

so that

$$F = 6.3 Re_g^{-0.3} Re_p^{-0.33}$$

Equation (34) also indicates that the gas Reynolds number has less of an effect on the heat-transfer coefficient of a gaseous suspension than on the heat-transfer coefficient of a pure gas (see eqs. (15), (17), and (25)).

The physical characteristics and size of the particles are accounted for by the dimensionless group Re_p , which shows that a reduction in the size of the solid particles will increase the heat-transfer coefficient for the same settling velocity. The correlation given by equation (34) applies in the range of variables $7000 < Re_g < 65\,000$, $5 < Re_p < 800$, $1 < \eta < 32$, $0.84 < \delta < 1.03$, and $12 < D/D_p < 133$.

In their paper, Gorbis and Bakhtiozin claim to have correlated the data of Farbar and Morley; however, it should be noted, that Gorbis in using his correlation assumed a value of 150 microns for the diameter of the particles (the smallest particle size for which his correlation is applicable) used in the Farbar and Morley work, whereas the actual average diameter of the particles was about 50 microns. Using the correct particle diameter (50μ) in his correlation does not bring close agreement with the data of Farbar and Morley. This lack of agreement could indicate that Gorbis' correlation should not be extrapolated to particle sizes smaller than 150 microns.

Tien. - An analytical study of heat transfer from a turbulently flowing fluid-solid mixture in a pipe was done by Tien (ref. 22). By making certain assumptions, Tien was able to solve the energy equations for both the solid and the fluid analytically. Tien's analytical solution indicates that the effect of the solid particles on the heat-transfer coefficient is governed by the factor $\delta \eta$. This fact was also shown in the correlations presented by Gorbis (ref. 6) and Schluderberg, et al. (ref. 18). Tien's results are applicable only to solid loading ratios less than one and show that in this range the heat-transfer coefficient varies linearly with loading ratio. The actual increase in heat-

transfer coefficient, however, is so slight that the advantages of adding solids in this range are negligible.

Tien and Quan. - In order to verify Tien's analytical solution (ref. 22), Tien and Quan (ref. 23) carried out an experimental heat-transfer study using air, and 30- and 200-micron glass and lead particles. Gas Reynolds numbers were set at 15 000 and 30 000, and loading ratios were varied only between 0 and 3. The experimental results showed a peculiar feature: the Nusselt number first decreased and then increased as the loading ratio was increased for fixed gas Reynolds number and particle size. This feature was not indicated by Tien's analytical study, and the authors proposed that the decrease in Nusselt number is due to the distortion of the gas flow field by the presence of solid particles that was not accounted for in the theory.

Tien and Quan did not present a correlation of their data. Qualitatively, however, they found that the heat-transfer coefficient ratio decreases with an increase in gas Reynolds number, which is in agreement with Farbar and Morley, Gorbis and Bakhtiozin, Farbar and Depew, and Danziger. They also found that the heat-transfer coefficient ratio increases with δ , as predicted by Tien's analytical work and Gorbis' correlation, and decreases with an increase in particle size, as was found by Gorbis, and Farbar and Depew.

Tien and Quan also measured the maximum temperature difference between particles and fluids and found this to be about 20° F for the 200-micron particles, but only 3° F for the 30-micron particles. Thus, small particles are likely to have a negligible temperature lag, whereas a suspension of large particles is likely to be far from equilibrium conditions.

Mickley and Trilling. - Mickley and Trilling (ref. 24) conducted their research to determine the effect of the presence of solids on heat-transfer conditions at surfaces in contact with a fluidized gas-solid mixture. The experimental work was carried out in vertical fluidized beds 1 to 4 inches in diameter. The fluidized mixture consisted of glass spheres with particle diameters ranging from 40 to 450 microns suspended in an upward flowing stream of air at superficial velocities varying between 0.8 and 15 feet per second. Several groups of particles of fixed size were tested in this range.

The work of Mickley and Trilling was carried out in fluidized beds, and hence the direct validity or quantitative applicability of their results is questionable for use with suspensions; however, the important trends and variations observed in their data might be qualitatively applicable to solid suspensions flowing in tubes.

Mickley and Trilling found that for the four groups of large-size particles (150 to 450 μ), the slope of the line that resulted when the log of the heat-transfer coefficient was plotted against the log of the particle concentration was relatively constant at a value between 0.46 and 0.55. This value is in good agreement with the suspension work of Farbar and Morley, Danziger, and Schluderberg. They also found that at any given

concentration, the heat-transfer coefficient varies at a rate inversely proportional to the 0.61 to 0.74 power of the particle diameter for the larger sized particles. However, this effect of particle diameter on heat-transfer coefficient decreased considerably for the smaller sized particles ($D_p < 150\mu$). This behavior was attributed to agglomeration of the smaller sized particles.

List. - The final heat-transfer study that will be reported in this technical note was done by List (ref. 25). List determined heat-transfer coefficients for four sizes of glass beads and two sizes of copper shot transported by air in a vertical heating section. The mixtures were electrically heated with an internal rod heating element. The solid flow rate for a given run was set by choosing one of a set of cone-shaped nozzles, precalibrated by determining the average weight of the solids delivered under static conditions. The smallest bead used was 51 microns in diameter, about the same size as the catalyst used by Farbar and Morley and by Danziger. List's data showed that h_s was inversely proportional to the solid particle size to the 0.04 to 0.09 power. At low velocities, the effect of particle size on h_s was found to increase. Mickley and Trilling found that h_s varied inversely proportional to the 0.61 to 0.74 power of particle size. Indications are therefore that as the velocity increases from that of a fluidized bed to that of suspension flow, the effect of particle size becomes smaller.

Although List reports extensive data that would be valuable to any heat-transfer study, Danziger (ref. 5) believed List's data to be unreliable because the solid inlet nozzles were calibrated at static conditions rather than at dynamic conditions. Therefore, the data of List have not been used in the attempt to find an overall correlation.

Correlations

From the literature cited, it is apparent that the important parameters that determine heat transfer in a gas-solid suspension are the loading ratio η , the ratio of specific heat of the particles to the specific heat of the gas δ , the particle diameter D_p , and the gas Reynolds number Re_g . The effect of each of these parameters on the h_s/h_g ratio will now be studied in more detail based on the results of the aforementioned studies, and an attempt will then be made to establish a consistent workable correlation.

Effect of loading ratio η and specific heat ratio δ . - The heat-transfer correlations deduced in the references cited are summarized below in terms of the heat-transfer coefficient ratio:

Farbar and Morley:

$$\frac{h_s}{h_g} = 6.8 Re_g^{-0.2} \eta^{0.45} \quad (15)$$

Danziger:

$$\frac{h_s}{h_g} = 3.7 \operatorname{Re}_g^{-0.14} \eta^{0.45} \quad (17)$$

Schluderberg:

$$\frac{h_s}{h_g} = 0.78 (1 + \delta\eta)^{0.45} \quad (19)$$

The Franklin Institute:

$$\frac{h_s}{h_g} = 16.9 \operatorname{Re}_g^{-0.3} (1 + \delta\eta)^{0.45} \quad (25)$$

Gorbis and Bakhtiozin:

$$\frac{h_s}{h_g} = 1 + \left(6.3 \operatorname{Re}_g^{-0.3} \operatorname{Re}_p^{-0.33} \right) \delta\eta \quad (34)$$

The one fact that finds unanimous agreement from these equations is that the heat-transfer coefficient ratio increases as the loading ratio increases although three different forms of the loading ratio dependence are suggested. If all of the other parameters of the system are held constant, these forms may be written as

$$\frac{h_s}{h_g} = k_1 \eta^a \quad (35)$$

$$\frac{h_s}{h_g} = k_2 (1 + k_3 \eta)^b \quad (36)$$

$$\frac{h_s}{h_g} = 1 + k_4 \eta \quad (37)$$

where the k 's are, in general, functions of other variables, and a and b are positive

exponents less than one.

In the range of loading ratios of primary interest ($\eta < 10$), there has been little experimental work done to determine the effect of δ on h_s/h_g although it almost certainly exerts a strong influence on the heat-transfer coefficient ratio. The only work where δ has been specifically investigated experimentally is that of Tien and Quan at low loading ratios. Their work qualitatively indicates that h_s/h_g increases with an increase in δ . Tien's analytical work indicates that the factor $\delta\eta$ should be treated as a unit, which also is predicted by the Reynolds analogy as presented by Gorbis. Schluderberg and the Franklin Institute also use the factor $\delta\eta$ as a unit in their correlations. Although the available data are very limited as to the effect of δ , it seems reasonable to assume that the factor $\delta\eta$, which can be thought of as a weighted specific heat ratio, should appear as a unit. Thus, equations (15) and (17) are rewritten for the respective gases and particles used:

$$\frac{h_s}{h_g} = 6.4 \text{ Re}^{-0.2} (\delta\eta)^{0.45} \quad (38)$$

and

$$\frac{h_s}{h_g} = 4.0 \text{ Re}^{-0.14} (\delta\eta)^{0.45} \quad (39)$$

It should be noted at this point that some disagreement exists concerning the value of δ of the silica-alumina catalyst used by both Danziger and by Farbar and Morley (table I). The procedure utilized in the preceding paragraphs, however, negates any

possible errors introduced by an incorrect δ in obtaining their respective constants since the constants appearing in equations (38) and (39) are now presumably independent of δ .

In order to see how closely the correlations agree with one another, the heat-transfer coefficient ratio as predicted by equations (38), (39), (25), and (34) was plotted against $\delta\eta$ in figure 6. The values are plotted for a gas Reynolds number arbitrarily set at 20 000 and for the smallest allowable particle diameter

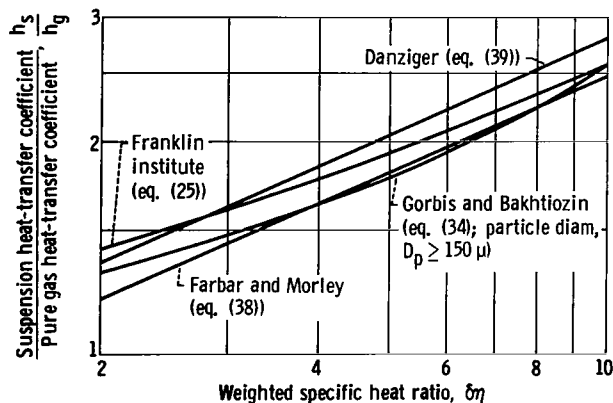


Figure 6. - Effect of weighted specific heat ratio on heat-transfer coefficient ratio. Gas Reynolds number, 20 000.

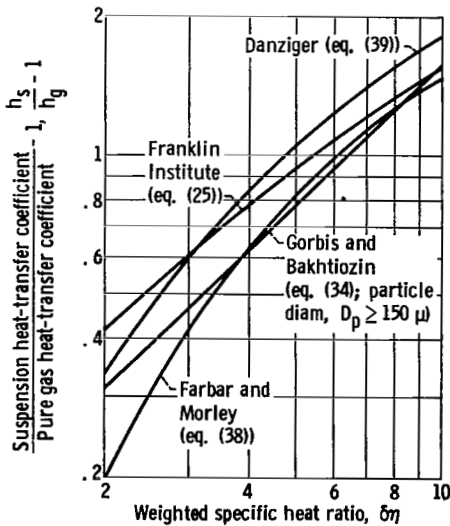


Figure 7. - Effect of weighted specific heat ratio on heat-transfer coefficient ratio. Gas Reynolds number, 20 000.

(150 μ) in the Gorbis and Bakhtiozin correlation. The figure shows close agreement between all the correlations indicating that the form (eqs. (38) and (39))

$$\frac{h_s}{h_g} = k'_1 (\delta\eta)^{0.45} \quad (40)$$

is a good representative correlation. On the other hand, a plot of $(h_s/h_g) - 1$ against $\delta\eta$, obtained from the correlation equations as presented in figure 7, also shows fairly good agreement between all the correlations. This agreement indicates that an equation of the form

$$\frac{h_s}{h_g} = 1 + k'_4 \delta\eta \quad (41)$$

is also a good representative correlation in the same range. Thus it seems that either equation (40) or (41) is applicable in the range of interest $2 < \eta < 10$. However, while h_s/h_g in equation (41) reduces to unity as it should when $\eta \rightarrow 0$, equation (40) does not. Equation (41), however, gives high values for h_s/h_g when compared to Danziger's experimental data at loading ratios greater than 15, whereas equation (40) is in agreement with Danziger's data in the entire loading ratio range.

The form of equation (25)

$$\frac{h_s}{h_g} = k'_2 (1 + \delta\eta)^{0.45} \quad (42)$$

seems to offer no advantage over the other two forms and will be abandoned.

Effect of particle diameter. - Another parameter of importance on which little experimental or analytical work is available is the particle diameter. It is generally acknowledged that there should be some decrease in the heat-transfer coefficient ratio as the particle diameter is increased. The experimental works that attempted to find the particle diameter dependence are the work of Gorbis and Bakhtiozin, Farbar and Depew, List, and the work of Mickley and Trilling with fluidized beds.

Gorbis and Bakhtiozin expressed the particle diameter dependence in terms of the dimensionless group Re_p (eq. (34)). This group can be expressed specifically in terms

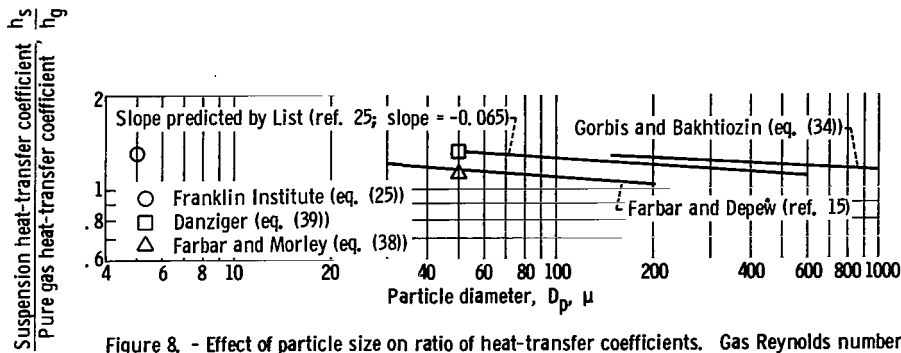


Figure 8. - Effect of particle size on ratio of heat-transfer coefficients. Gas Reynolds number, 26 500; weighted specific heat ratio, 2.

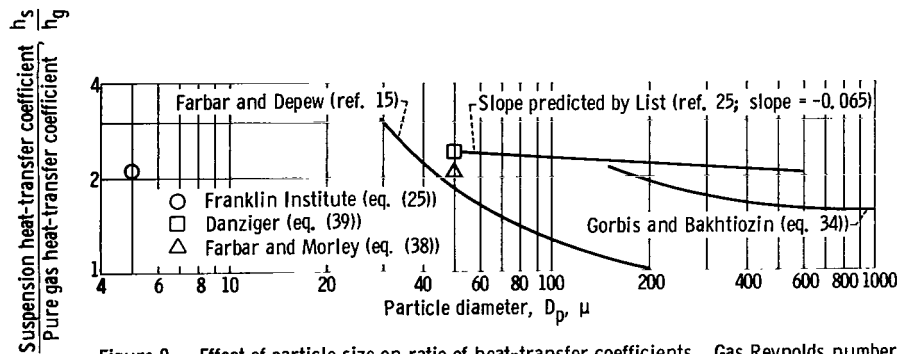


Figure 9. - Effect of particle size on ratio of heat-transfer coefficients. Gas Reynolds number, 26 500; weighted specific heat ratio, 8.

of particle diameter by eliminating V_{ps} explicitly with the help of standard drag coefficient data (ref. 21) and shows that particle diameter exerts a small influence on h_s/h_g . List's work (ref. 25) indicates that the heat-transfer coefficient ratio varies inversely with the 0.04 to 0.09 power of the particle diameter. Farbar and Depew show a much larger effect of particle diameter and indicate that with particles of 200-micron diameter the heat-transfer coefficient of a suspension is essentially the same as that of a pure gas. Mickley and Trilling (fluidized beds) suggest that h_s/h_g varies inversely with the 0.6 to 0.7 power of the particle diameter for particles greater than 150 microns and that the effect is smaller for smaller particles. This contention is in contradiction with the results of Gorbis and Bakhtiozin and List; however, this large particle diameter dependence is believed attributable to the low velocities encountered in fluidized beds.

A plot of h_s/h_g against D_p at a constant gas Reynolds number of 26 500 is presented in figure 8 for a value of $\delta\eta$ equal to 2 and in figure 9 for a value of $\delta\eta$ equal to 8. The correlations of Farbar and Morley, Danziger, and Schluderberg (or the Franklin Institute) appear as single points on these plots since these correlations were each based on only one particle diameter. List's work is represented by a line of average slope -0.065 and was arbitrarily passed through Danziger's result since List's smallest particle size was 50 microns and he presented no general correlation for his

work. Farbar and Depew's experimental results and Gorbis's correlation are also presented in the figures within their ranges of applicability. It should be pointed out that Gorbis's correlation, in particular, should not be extrapolated to particle diameters below 150 microns especially at high $\delta\eta$ since the correlation shows a rapid rise in slope at this point, which is inconsistent with the experimental data in the low particle diameter range. As can be seen from the figures, with the exception of Farbar and Depew's data, at high $\delta\eta$ the effect of particle diameter is indicated to be small in the entire particle diameter range from 5 to 1000 microns.

For application in a Brayton cycle and other pumped circuits the particle diameter should be kept as small as possible to prevent surface erosion and any appreciable lag between the particle and gas in the rotating equipment; yet the particle diameter must be large enough to avoid stability problems. Stability problems arise if the particles separate from the gas stream and adhere to the boundary surface of the heat-transfer equipment because of a thermal gradient. For example, a visual inspection of Schluderberg's experimental loop showed that the gas suspension was remarkably free of erosion, plugging, or particle adherence to system surfaces except on the cooling surfaces of the loop where graphite particles were found to plate out. The instability of the suspension in these areas was caused by an anisotropic Brownian particle motion in the direction of the decreasing temperature gradient. Recent information obtained from the Bureau of Mines (ref. 26) indicates that the use of spherical graphite particles larger than 10 microns will minimize the stability problem. Thus, the range of particle diameters of interest for Brayton cycle and related work is of the order of 10 to 50 microns. In this range there appears to be no appreciable effect of particle diameter on the ratio h_s/h_g .

Effect of gas Reynolds number. - Most of the literature indicates that a decrease of h_s/h_g should result when there is an increase in gas Reynolds number. This decrease can be explained by a reduction in the relative turbulence-producing effect of the motion of the solid particles in the gaseous flow, the turbulence of which increases with an increase in the Reynolds number.

Plots of h_s/h_g against gas Reynolds number for two representative values of $\delta\eta$ of 2 and 10 are shown in figures 10 and 11, respectively. The figures show close agreements between the correlations of Farbar and Morley (eq. (38)), Danziger (eq. (39)), Schluderberg (eq. (25)), and Gorbis and Bakhtiozin (eq. (34)) for 150-micron particles, and the data of Farbar and Depew for 30-micron particles. The data of Farbar and Depew does not extend to $\delta\eta = 10$ and therefore could not be plotted in figure 11. A representative average slope of these curves can be taken as -0.21, which is in good agreement with that predicted by Farbar and Morley's correlation, as shown by the faired dashed lines in figures 10 and 11.

Good agreement among the various correlations can also be obtained in terms of $(h_s/h_g) - 1$, as shown by figure 12. Figure 12 is a plot of $(h_s/h_g) - 1$ against Re_g for

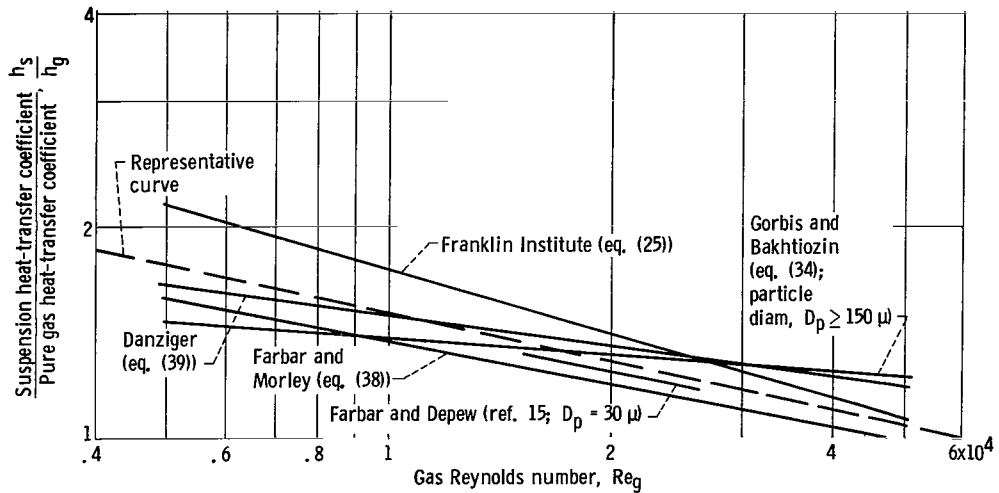


Figure 10. - Effect of gas Reynolds number on heat-transfer coefficient ratio. Weighted specific heat ratio, 2.

$\delta\eta = 10$. An average representative slope of these curves, as indicated by the faired dashed line, is -0.32 , which is in good agreement with Gorbis's correlation.

Final form of correlation. - The final forms of equations (40) and (41) based on the representative (dashed) lines drawn in figures 10, 11, and 12 appear as follows

$$\frac{h_s}{h_g} = 7.6 Re_g^{-0.21} (\delta\eta)^{0.45} \quad (43)$$

$$\frac{h_s}{h_g} = 1 + 4.0 Re_g^{-0.32} \delta\eta \quad (44)$$

These equations have been plotted against $\delta\eta$ in figure 13 for three different gas Reynolds numbers. As can be seen from the figure, the agreement between the correlations in the range of $2 < \eta < 10$ is good.

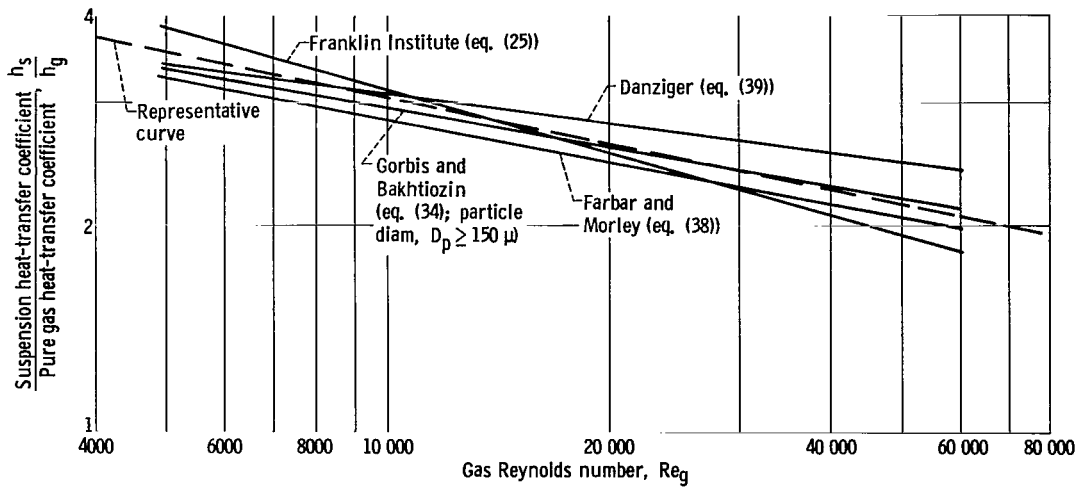


Figure 11. - Effect of gas Reynolds number on heat-transfer coefficient ratio. Weighted specific heat ratio, 10.

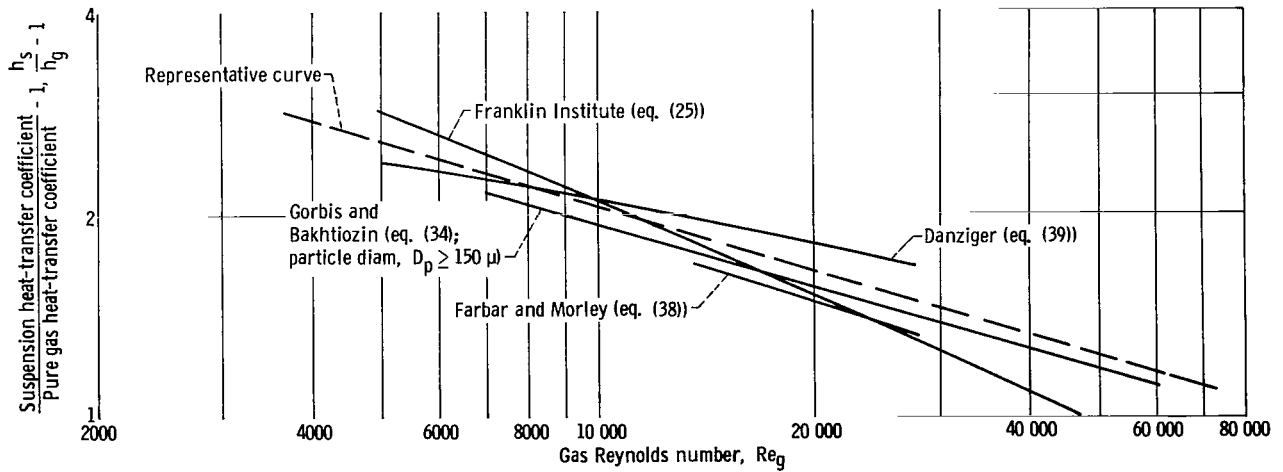


Figure 12. - Effect of gas Reynolds number on heat-transfer coefficient ratio factor. Weighted specific heat ratio, 10.

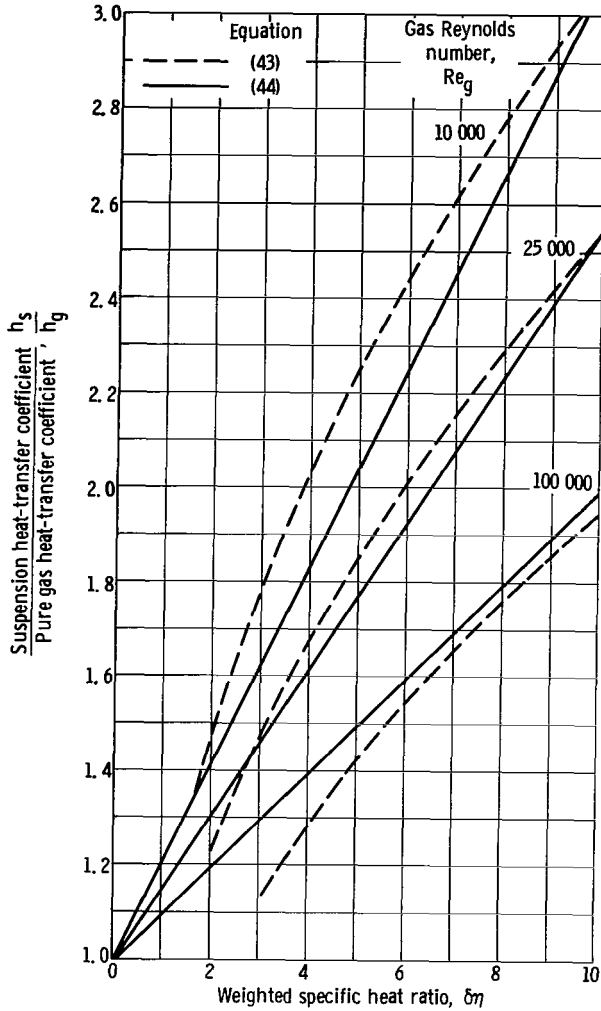


Figure 13. - Comparison of two final heat-transfer coefficient correlations at various gas Reynolds numbers.

These correlations should be applicable in the range of gas Reynolds numbers from 5000 to 100 000, $\delta\eta$ between 2 and 10, and to particle diameters between 5 and 50 microns. As indicated in the preceding section, the particle diameter effect in this range has been regarded as negligible.

PRESSURE DROP

In view of the widespread use of gas-solid conveying in a variety of industries, it would be expected that the friction and pressure drop flow phenomena would be well defined and understood. Investigation of the literature, however, indicated that the prediction of pressure loss in gas-solid suspensions is still an empirical art. In the ensuing sections an attempt will be made to find a working correlation that will predict pressure drop of suspension flow.

Pure Gas Relations

For a pure gas, the pressure drop for

flow in a pipe is given by the Fanning equation

$$\Delta P_g = 2f_g \frac{L}{D} \rho_g \frac{V_g^2}{g_c} \quad (31c)$$

where the value of the gas friction factor f_g is well established for all flow regimes. For fully developed turbulent flow in smooth tubes under adiabatic conditions

$$f_g \cong 0.046 Re_g^{-0.2} \quad \text{for } 10\,000 < Re_g < 100\,000 \quad (45)$$

It would be convenient to develop an equation similar in form to the Fanning equation

with appropriate modifications to predict the pressure drop of a gas-solid suspension. The friction factor for flow of a gas-solid suspension, however, is not expected to be merely a simple function of gas Reynolds number but may depend on other variables such as loading ratio η and particle diameter D_p .

Flow Regimes

There have been a number of studies made to determine the effect of the suspension flow patterns (gas and solid velocity profiles) on the pressure drop of suspensions (refs. 27, 28, and 29). The most recent effort to determine the mechanism of gas-solid flow in tubes is the work of Peskin and Dwyer (ref. 30). From their experimental work they have concluded that gas-solid flow can be divided into the four following distinct flow regimes:

(1) Particles cause viscous disturbances and increase the size of the laminar sub-layer and thus a decrease in the shearing stress at the wall. In this case, the particles are very close together but occupy a small volume.

(2) Particles cause mostly viscous disturbances, but are too far apart to affect the gas velocity profile and hence the laminar sublayer. The shearing stress at the wall is unchanged.

(3) Particles cause inertial disturbances that alter the gas velocity profile and decrease the size of the laminar sublayer. In this case, the wall shearing stress increases.

(4) Particles occupy a large volume and change the geometry of the flow. This situation is similar to the flow in packed beds.

It appears therefore that the variation of the friction factor of a gas-solid suspension with loading ratio and other parameters may depend on which flow regime is applicable and may not be generalized for all gas-solid flows.

Analytical Models

Several analytical models for describing the pressure loss of gas-solid suspensions are available based on the assumption that the mixture flows at a velocity greater than either the saltation velocity in horizontal tubes (the lowest possible velocity required to keep a specific particle in suspension) or the choking velocity in vertical tubes (the minimum velocity required to prevent the suspension from being transported up the tube in slug flow). Under these conditions the pressure drop for the general flow of gas-solid suspensions through tubes is considered to be composed of the following six forces:

- (1) The friction of the gas against the pipe wall
- (2) The friction between the solids and the pipe wall
- (3) The drag force required to move the solids through the pipe
- (4) The force required to accelerate the gas to its equilibrium velocity profile
- (5) The force required to accelerate the particles to their equilibrium velocity
- (6) In vertical tubes, the force required to support the weight of solids and gas

The following models were employed to determine pressure drop in a gas-solid suspension and are based on the inclusion of the preceding forces in varying degrees and forms.

Drag coefficient model. - Zenz and Othmer (ref. 21) present the following equation proposed by Hinkle (ref. 31) for predicting the pressure drop of a dilute suspension:

$$\Delta P_s = \frac{V_g^2 \rho_g}{2g_c} + \frac{\rho'_p V_p^2}{g_c} + \frac{2f_g \rho_g V_g^2 L}{g_c D} + \frac{2f'_p \rho'_p V_p^2 L}{g_c D} + \rho'_p L \quad (46)$$

$\underbrace{\hspace{10em}}$ Fluid accelera- tion	$\underbrace{\hspace{10em}}$ Particle accelera- tion	$\underbrace{\hspace{10em}}$ Fluid to pipe friction	$\underbrace{\hspace{10em}}$ Particle friction and drag	$\underbrace{\hspace{10em}}$ Weight of particles (Vertical tubes only)
--	---	--	---	--

where

ρ'_p density of solid, $\rho_s - \rho_g$, lb solid/ft³ mixture

f'_p particle friction factor based on particle velocity and particle density in mixture

For a horizontal tube of constant diameter that is of sufficient length so that acceleration forces can be neglected (particles and fluid having reached their respective equilibrium velocities), this equation reduces to

$$\Delta P_s = \frac{2f_g \rho_g V_g^2 L}{g_c D} + \frac{2f'_p \rho'_p V_p^2 L}{g_c D} \quad (47)$$

or with the use of equation (31c)

$$\frac{\Delta P_s}{\Delta P_g} = 1 + \frac{f'_p \rho'_p V_p^2}{f_g \rho_g V_g^2} \quad (48)$$

But since η is the ratio of the mass flow rate of particles to the mass flow rate of pure gas

$$\eta = \frac{W_p}{W_g} = \frac{\rho'_p V_p}{\rho_g V_g} \quad (49)$$

then

$$\frac{\Delta P_s}{\Delta P_g} = 1 + \frac{f'_p V_p}{f_g V_g} \eta \quad (50)$$

Equation (50) is simply another form of the Gasterstadt relation (eq. (32)) where $F = f'_p V_p / f_g V_g$. Before equation (50) can be used to determine ΔP_s , however, a means of obtaining both f'_p and V_p is necessary.

For particle sizes showing a significant velocity lag or slip between the particles and the transporting fluid, Hinkle (ref. 31) assumed the pressure drop due to the presence of the particles to be caused entirely by the drag of the fluid on the particles. In this case, the particle-to-wall friction can be neglected in comparison with the drag. Based on this assumption, the pressure drop due to the particle drag is

$$\frac{2f'_p \rho'_p V_p^2 L}{g_c D} = \frac{n C_D \rho_g (V_g - V_p)^2 \pi D_p^2 L}{8 g_c}$$

or

$$f'_p = \frac{n C_D}{16} \frac{\rho_g}{\rho'_p} \frac{(V_g - V_p)^2}{V_p^2} \pi D_p^2 D \quad (51)$$

where n is the number of particles per cubic foot of mixture and C_D is the standard drag coefficient for spherical particles defined by

$$C_D = \frac{8 F_D g_c}{\pi D_p^2 \rho_g (V_g - V_p)^2}$$

where F_D is the drag force and $V_g - V_p$ is the relative velocity between the gas and particle.

Since

$$n = \frac{6\rho'_p}{\rho_p \pi D_p^3}$$

then

$$f'_p = \frac{3}{8} \frac{C_D \rho_g (V_g - V_p)^2 D}{\rho_p V_p^2 D_p} \quad (52)$$

In order to employ this model the particle velocity must be known. If experimental values of V_p are not available, the particle velocity can be crudely estimated by assuming V_p to be equal to $V_g - V_{ps}$ where the terminal settling velocity V_{ps} can be obtained from the standard drag coefficient - Reynolds number correlation (ref. 21): however, the attendant difficulty of obtaining an accurate particle velocity makes this model difficult to apply in obtaining the particle friction factor. In addition, the effect of particle-to-wall friction has been entirely omitted. For example, for particles small enough to show no slip ($V_g = V_p$), this model would predict no additional pressure drop due to the particles.

Equivalent friction factor model. - The inherent disadvantages of the previous model indicate the desirability of having a simpler model to predict suspension pressure drops. The equivalent friction factor model simply defines the pressure drop of the suspension as

$$\Delta P_s = 2f'_s \rho_g \frac{L}{D} \frac{V_s^2}{g_c} \quad (31a)$$

where f'_s is an equivalent suspension friction factor and ρ_g is the density of the gas in the suspension. If this equation is divided by the Fanning equation for the same gas conditions in the tube then

$$\frac{\Delta P_s}{\Delta P_g} = \frac{f'_s}{f_g} \quad (31d)$$

An alternative definition of the equivalent friction factor based on suspension density is given by

$$\Delta P_s = 2f_s \rho_s \frac{L}{D} \frac{V_s^2}{g_c} \quad (53)$$

Thus f'_s is related to f_s by the relation

$$f'_s = f_s \frac{\rho_s}{\rho_g} = f_s (1 + \eta) \quad (54)$$

In both cases, f_s/f_g as well as f'_s/f_g are presumably functions of loading ratio, gas Reynolds number, particle diameter, and other properties of the suspension that must be determined experimentally.

Reynolds analogy. - Another approach to the determination of the suspension friction factor is the use of the Reynolds analogy. The Reynolds analogy is of historical importance as the first recognition of analogous behavior of momentum- and heat-transfer rates. The Reynolds analogy can be applied to gas-particle suspensions if the suspension is assumed to behave as a homogeneous fluid and if an accurate relation for the heat-transfer coefficient of suspensions is assumed available.

By applying the Reynolds analogy to the gas and solid phases separately, as was done by Gorbis in reference 6, the relation between f_p/f_g and h_s/h_g is obtained:

$$\frac{h_s}{h_g} = 1 + \frac{\delta f_p}{f_g} \quad (30)$$

By definition in this development

$$f'_s = f_g + f_p \quad (31b)$$

where f'_s is defined by equation (31a), f_p is defined by equation (28), and f_g is defined by equation (31c). Thus with the use of equation (30)

$$\frac{f'_s}{f_g} = 1 + \frac{1}{\delta} \left(\frac{h_s}{h_g} - 1 \right) \quad (55)$$

The Reynolds analogy can also be applied by comparing the gas directly with the suspension rather than by superposition of the gas and solid phases as was done previously. The Reynolds analogy yields

$$\frac{h_g}{\rho_g (C_p)_g V_g} = \frac{f_g}{2} \quad \text{for the gas} \quad (26)$$

and

$$\frac{h_s}{\rho_s (C_p)_s V_s} = \frac{f_s}{2} \quad \text{for the suspension}$$

where f_s is the equivalent friction factor defined by equation (53). Dividing f_s by f_g and assuming equal volumetric rates of flow so that $V_g = V_s$ give

$$\frac{f_s}{f_g} = \frac{h_s}{h_g} \left[\frac{\rho_g (C_p)_g}{\rho_s (C_p)_s} \right]$$

In terms of loading ratio η for equal velocities (eq. (1c)) and ratio of specific heats δ (eq. (3)),

$$\frac{f_s}{f_g} = \frac{h_s}{h_g} \frac{1}{1 + \eta} \frac{1 + \eta}{1 + \delta\eta}$$

or

$$\frac{f_s}{f_g} = \frac{h_s}{h_g} \frac{1}{1 + \delta\eta} \quad (56)$$

With the use of equation (54),

$$\frac{f'_s}{f_g} = \frac{h_s}{h_g} \frac{1 + \eta}{1 + \delta\eta} \quad (57)$$

Thus, either equation (55) or (57) can be used to relate the equivalent friction factor of the suspension to the heat-transfer coefficient of the suspension, depending on the method of application of the Reynolds analogy. When $\delta = 1$, both forms reduce to the simple expression

$$\frac{f'_s}{f_g} = \frac{h_s}{h_g} \quad (58)$$

Thus, once a workable relation for h_s/h_g is accepted, a reasonable relation for f'_s/f_g might also result.

Eddy viscosity model. - In a recent paper, Julian and Dukler (ref. 32) attempted to find a correlation for pressure drop caused by a gas-solid suspension by use of an eddy viscosity model. In their work, they suggest that for dilute-phase transport the solids make their presence felt primarily by modifying the local turbulence in the gas phase, increasing the turbulent fluctuations, mixing length, and eddy viscosity, and consequently, frictional pressure drop.

Julian and Dukler's analysis is based on a modification of Gill and Scher's expression (ref. 33) for the eddy viscosity ϵ' of a pure fluid flowing through a tube. Gill and Scher's equation is

$$\epsilon' = K^2 y^2 \left(1 - e^{-\frac{2\phi y}{D}} \right)^2 \frac{dV_g}{dy} \quad (59)$$

where K is the universal von Kármán constant for pure gas originally reported as 0.4 and found by Deissler (ref. 34) to be closer to 0.36. Julian and Dukler modified the Gill and Scher equation to take into account the effect of particles by redefining.

$$K = k(1 + \eta)^m \quad (60)$$

The unknown constants k and m are to be determined from experimental data. By a trial-and-error procedure, using the experimental data of six different investigators (refs. 31 and 35 to 39) Julian and Dukler were able to show that a log plot of K against $1 + \eta$ is essentially a straight line as predicted by their model. For loading ratios below 12 they found that

$$K = 0.36(1 + \eta)^{0.25} \quad (61)$$

and for loading ratios above 12

$$K = 0.11(1 + \eta)^{0.8} \quad (62)$$

Equation (61) is especially encouraging since at $\eta = 0$, K reduces to 0.36, which is the accepted value for flow of a particle-free gas.

Since the eddy viscosity can be readily related to the equivalent friction factor f'_s of equation (31a) (ref. 32), Julian and Dukler's model can be used to obtain suspension pressure drops. These results are discussed in a later section (Correlations section).

Data Sources

In order to evaluate fully the validity of the aforementioned models and mechanisms, an extensive literature search was undertaken. The purpose of this literature search was to uncover experimentally obtained data and correlations capable of being used in this evaluation procedure. A brief review of the literature available in this field is presented in the following sections, and a summary of the operating conditions and the physical properties of gases and solids used in each experiment is presented in table II. The

TABLE II. - SUMMARY OF OPERATING CONDITIONS USED IN PRESSURE DROP WORK CITED

Particle	Gas	Particle diameter, D_p , μ	Loading ratio, η	Gas velocity, V_g , ft/sec	Equivalent tube diameter, D , in.	Gas Reynolds number, Re_g	Tube length, L , in.	Source
Glass	Air	80, 110	0 to 4	100	3	132 000	36	Peskin and Dwyer (ref. 30)
Glass	Air	80, 110	0 to 14	60 to 100	3	100 000 to 150 000	36	Peskin (ref. 40)
Glass	Air	36, 97	0.7 to 7	10 to 90	0.5	10 000 to 60 000	158	Mehta, Smith, and Comings (ref. 41)
Alumina-silica catalyst	Air	10 to 220 (avg 50)	0 to 16	50 to 150	0.69	17 000 to 50 000	87	Farbar (ref. 42)
Millet, peas, turnip seeds, pine kernels and sunflower seeds	Air	1280, 5760, 1900, 5850, 4000, 8400	0 to 15	65 to 130	5	110 000 to 321 000	80	Dogin and Lebedev (ref. 43)
Sand, clover seed, wheat	Air	200, 730, 330, 1150, 440, 4000	0.6 to 41.6	35 to 150	0.5	9000 to 39 000	300	Vogt and White (ref. 44)

experiments were conducted at room temperature with pressure levels ranging from 1 to 3 atmospheres among the various data sources.

Peskin and Dwyer. - In order to verify the drag coefficient model (eqs. (50) and (52)), Peskin and Dwyer (ref. 30) measured pressure drop and both fluid and particle velocity profiles for loading ratios up to 4 by using 80- and 110-micron-diameter glass particles in air in a 3-inch-square duct. For these small, relatively widely spaced particles (regime 2), Peskin found that the flow disturbances caused by the particles are entirely viscous since the particles because of their small size do not possess enough inertia in themselves to cause an inertial disturbance in the gas. Also, because of the relatively large spacing between the particles, the gas velocity profile was found to revert back to a universal profile between the particles. The average velocity of the particles, however, showed a large deviation from the velocity calculated by using the standard drag coefficient for the settling velocity; that is, on the basis of the experimentally measured particle velocity, the drag coefficient C_D calculated from the pressure drop measurements was much higher than that predicted from the standard correlation (eq. (52)). Peskin attributes the high drag coefficients to the added drag of the longitudinal component of the turbulence of the fluid rather than to shortcomings in the assumed model. Because of the disparity between the model and Peskin's data, the drag coefficient model does not appear useful for predicting suspension pressure drops.

Peskin. - In another investigation, Peskin (ref. 40) also correlated some of his pressure drop data in terms of the equivalent friction factor f_s defined by equation (53). Sets of curves of f_s against gas Reynolds number were obtained for two different glass particle sizes (80- and 110- μ diam.) at Reynolds numbers of 100 000 to 150 000 and loading ratios up to 14 in a 3-inch-square duct. The faired variations of these curves after conversion to f'_s are presented in figure 14 and show that in all cases the equivalent

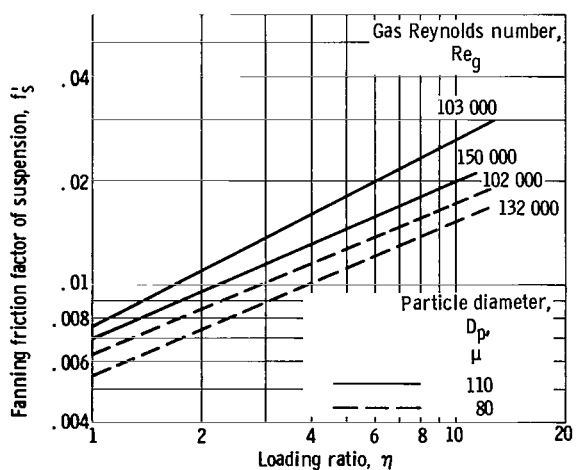


Figure 14. - Fanning friction factor of suspension as function of loading ratio as computed from faired data of reference 40.

friction factor f'_s increases with increasing solids loading ratio and with decreasing gas Reynolds number. In addition, the curves indicate that at a given loading ratio and Reynolds number, the friction factor is smaller for the 80-micron particles than for the 110-micron particles. These results are contrary to the heat-transfer work discussed earlier (p. 23), where it was shown that heat-transfer coefficients tend to decrease slightly with increasing particle diameter. The effects of particle diameter on heat-transfer coefficients, however, may be different from the effects on friction factor

because of the velocity lags inherent with larger particles.

It should also be noted at this point that the results for the friction factor of the 110-micron particles are somewhat dubious in view of certain experimental inaccuracies in the runs for this particle size (private communication from R. L. Peskin). It is therefore conceivable that the large-particle-diameter effect reported by Peskin may not be correct.

Mehta, Smith, and Comings. - In the work of Mehta, Smith, and Comings (ref. 41), 36- and 97-micron-diameter glass beads were each suspended in air flowing through a 1/2-inch-diameter pipe. The gas Reynolds number was varied between 10 000 and 60 000, and the loading ratio was varied between 0.7 and 4.7 for the 36-micron particles and between 0.7 and 7.0 for the 97-micron particles. As a result of their study, the authors concluded that the pressure drop in air-solid transport systems is dependent upon the type of particle flow. The authors of reference 41 postulated that the 97-micron solids were primarily in "bouncing" flow, where the particles are in unsteady motion and frequently collide with the wall of the pipe. The 36-micron particles were assumed to be in suspension flow, where the particles flow in a suspended condition that is maintained by the finite slip velocity between the particles and the gas.

The authors attempted to correlate their data using the drag coefficient model (eq. (52)) with no success. They finally proposed a correlation based on a so-called mixture friction factor f_m defined by

$$\Delta P_s = \frac{f_m \frac{L}{D} V_g^2 \rho_g}{2g_c} \left[1 + \left(\frac{V_p}{V_g} \eta \right)^{a'} \right] \quad (63)$$

where a' is a constant chosen by the authors as 0.3 for the 36-micron particles and 1.0 for the 97-micron particles. Upon plotting f_m from their pressure drop data against gas Reynolds number, they found f_m to be roughly constant, or independent of solid flow rates, for both particle sizes at Reynolds numbers greater than 30 000. The average values of f_m were 0.016 for the 36-micron particles and 0.035 for 97-micron particles. At gas Reynolds numbers less than 30 000 these values increased as Re_g was decreased.

In Mehta's experiments, V_p/V_g for the 36-micron particles remained relatively constant at about 0.7, whereas for the 97-micron particles, V_p/V_g varied considerably (from about 0.22 to 0.67). The reason for this might be that the 97-micron particles were not fully accelerated when the pressure drop measurements were recorded, and this could therefore account for the much higher pressure drop observed with the 97-micron particles.

Dividing equation (63) by equation (31a) gives the following relation between f'_s and f'_m :

$$f'_s = \frac{f'_m}{4} \left[1 + \left(\frac{V_p}{V_g} \eta \right)^{a'} \right] \quad (64)$$

Substituting the constant values for f'_m suggested by the authors for each particle size gives

$$f'_s = 0.004 + 0.004 \left(\frac{V_p}{V_g} \eta \right)^{0.3} \quad \text{for 36-micron particles} \quad (65)$$

and

$$f'_s = 0.0088 + 0.0088 \frac{V_p}{V_g} \eta \quad \text{for 97-micron particles} \quad (66)$$

The correlations given by equations (65) and (66) are difficult to apply, however, inasmuch as they depend on the magnitude of the particle velocity, which is a difficult quantity to determine. In addition, the correlation is only applicable for $Re_g > 30\,000$ since at lower gas Reynolds numbers, f'_m was not found by the authors to remain constant.

A plot of f'_s against η for several values of Re_g calculated from the Mehta, Smith, and Comings original horizontal-flow data (for $\eta > 1$) is presented in figure 15. The curve deduced from their 36-micron particle correlation according to equation (65), with $V_p/V_g = 0.7$ and Re_g greater than 30 000, is included as a comparison (denoted by the dashed line). Faired lines through the data points indicate that f'_s varies with approximately the 0.4 to 0.5 power of η , whereas the correlation gives a smaller dependence on η . The figure also shows that f'_s decreases with increasing gas Reynolds number.

These slopes are in general agreement with the data of Peskin shown in figure 14.

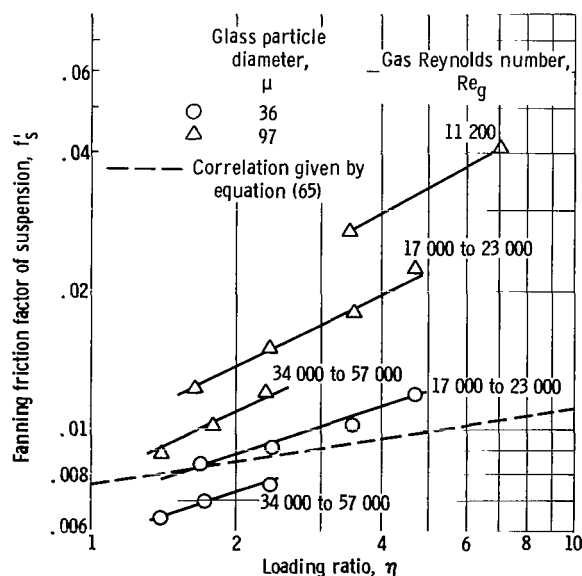


Figure 15. - Fanning friction factor of suspension as function of loading ratio as computed from data of reference 41.

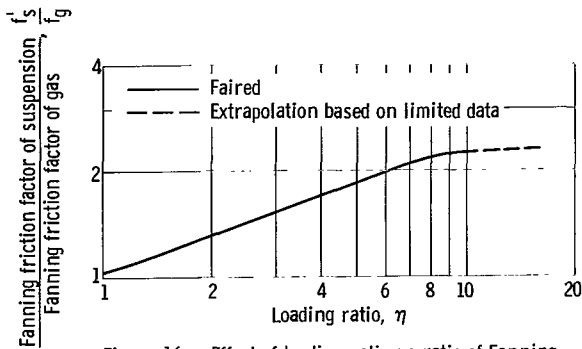


Figure 16. - Effect of loading ratio on ratio of Fanning friction factor of suspension to friction factor of gas (data from ref. 42.)

Farbar. - Farbar (ref. 42) measured the flow characteristics of solid-gas mixtures in both a horizontal and a vertical pipe 0.69 inch in diameter using a mixture consisting of silica -alumina catalyst and air. The loading ratio was varied between 0 and 16, and the particles had a size distribution varying from less than 10 microns to greater than 220 microns with an average diameter of 50 microns. The gas Reynolds number was varied between 17 000 and 50 000.

As a result of his studies, Farbar was able to report that $\Delta P_s/\Delta P_g = f'_s/f_g$ appeared to decrease when the gas flow rate Re_g was increased. Farbar also reported that $\Delta P_s/\Delta P_g$ increased as η was increased up to $\eta = 10$. Although his data above $\eta = 10$ were inadequate to establish a definite variation, he proposed that above this value the loading ratio no longer has an effect on the pressure drop of the suspension. It should be noted, however, that Farbar presents no correlation for his data and that the data (as given in his paper) for vertical transport are inconveniently presented because the author neglected to subtract the gravity head (the pressure drop caused by supporting a vertical column of suspension) from the total pressure drop to obtain the pressure drop caused by friction alone.

A plot of the curve given in Farbar's paper to represent the horizontal tube pressure drop data appears in figure 16. Although Farbar chose to draw a single line through all of his data, several lines could have been drawn for different values of Re_g . The curve shows, however, that f'_s/f_g varies approximately with the 0.42 power of η which is in good agreement with both the data of Mehta and Peskin.

Dogin and Lebedev. - In the work of Dogin and Lebedev (ref. 43), an attempt was made to determine the dependence of the friction factor f'_s of gas-solid suspensions on the loading ratio, flow velocity, specific weight, and dimensions of the particles being conveyed. The materials conveyed by air in a 5-inch-diameter horizontal pipe were millet ($D_p = 1900\mu$), peas ($D_p = 5760\mu$), turnip seeds ($D_p = 1280\mu$), wheat ($D_p = 4000\mu$), pine kernels ($D_p = 8400\mu$), and sunflower seeds ($D_p = 5850\mu$). The loading ratio was varied between 0 and 15, and the gas Reynolds numbers ranged from 110 000 to 321 000.

Dogin and Lebedev correlated their data by using the form presented by Gasterstadt

$$\frac{f'_s}{f_g} = 1 + F\eta \quad (32)$$

They observed that f'_s/f_g decreased as the flow velocity of the gas increased and found that $(f'_s/f_g) - 1$ was proportional to the ratio of the particle diameter to the pipe diameter taken to the 0.1 power and to the ratio of the densities of particle and gas ρ_p/ρ_g . The results of their investigation were summarized in their final correlation, which was given as

$$f'_s = f_g + \frac{A(D_p/D)^{0.1} (Re)_g^{0.4} \rho_p}{Fr_g^{0.5} \rho_g} \eta \quad (67a)$$

where Fr_g is the gas Froude number equal to V_g^2/gD , and A is a parameter that varied, depending on pipe roughness, between 1×10^{-6} and 2.2×10^{-6} in the experiments of Dogin and Lebedev.

Substituting equation (45) for f_g in equation (67a) indicates that for a given gas, particle density, and tube diameter

$$\frac{f'_s}{f_g} = 1 + C(D_p)^{0.1} (V_g)^{-0.4} \eta \quad (67b)$$

where C is a constant depending on the system. Equation (67b) shows that $(f'_s/f_g) - 1$ should increase slightly with particle diameter and increase with decreasing gas velocity. These trends are in good agreement with most of the literature.

Vogt and White. - In a paper by Vogt and White (ref. 44), the pressure differential required to produce steady flow of suspensions of sand ($D_p = 200, 330, 440, \text{ and } 730\mu$), clover seed ($D_p = 1150\mu$), and wheat ($D_p = 4000\mu$) in air through vertical and horizontal 1/2-inch-diameter pipes is presented. In their work, the loading ratio was varied between 0.6 and 41.6, and the gas Reynolds number ranged from 9000 to 39 000.

Vogt and White correlated their data in a form similar to that of Dogin and Lebedev

$$\frac{f'_s}{f_g} = 1 + B \left(\frac{D}{D_p} \right)^2 \left[\frac{\rho_g}{\rho_p} \frac{\eta}{(Re)_g} \right]^\ell \quad (68)$$

where B and ℓ are functions of the dimensionless group $Re_p(C_D)^{1/2}$. The large dependence of f'_s/f_g , on D/D_p in equation (68) has been disputed by Belden and Kassel (ref. 45) and others. Clark, et al. (ref. 38) reported that the sand runs might have been influenced by high electrostatic charges, which could have been responsible for the high pressure drops reported for these particles. Vogt and White's correlation and also all

TABLE III. - RANGE OF DATA USED BY JULIAN (REF. 32) FOR EVALUATION OF HIS MODEL

Particle	Gas	Particle diameter, D_p , μ	Loading ratio, η	Tube inside diameter, D , in.	Gas Reynolds number, Re_g	Source
Tenite, polystyrene, aluminum	Air	2290 to 6360	0.5 to 4.5	2, 3	178 000	Hinkle (ref. 31)
Glass	Air	25 to 200	0.5 to 3.5	0.7	13 500 to 27 400	Depew (ref. 39)
Cress seed	Air	1000	2.2 to 7.4	1	39 000 to 75 000	Clark, et al. (ref. 38)
Sand, glass, polystyrene	Air	435 to 940	0.4 to 12.1	1.5, 2	33 000 to 59 000	Helander (ref. 35)
Sand, cracking catalyst	Air, CO_2	200 to 510	0.5 to 36	0.25, 0.5	3700 to 11 000	Hariu and Molstad (ref. 37)
Glass, fertilizer, cress, brass, aluminum	Air	125 to 1525	1.6 to 16.5	1	43 000 to 78 000	Mitlin (ref. 36)

of his runs with sand are therefore highly questionable.

Other work. - Other important experimental studies involving pressure drop of gas-solid suspensions include the work of Hariu and Molstad (ref. 37); Clark, Charles, Richardson, and Newitt (ref. 38); Belden and Kassel (ref. 45); and the theses of Hinkle (ref. 31); Helander (ref. 35); Mitlin (ref. 36); and Depew (ref. 39). The experimental data from these works were thoroughly analyzed by Julian (ref. 46) in order to verify his eddy viscosity model. Some data were corrected for acceleration or static effects, and other inconsistent data were rejected (e.g., Belden and Kassel's data were rejected in their entirety). Therefore, a description of these works will not be repeated herein; however, a summary of the range of the operating variables involved appears in table III.

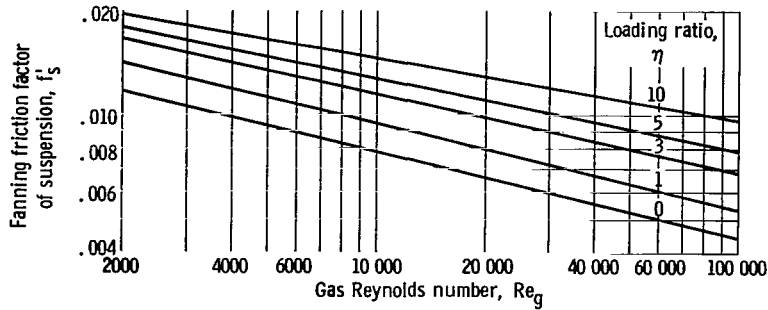


Figure 17. - Fanning friction factor of suspension as function of gas Reynolds number as predicted by reference 32.

Correlations

The object of this section is to obtain a working correlation that is descriptive of the available data and possesses the simplest form for ease of application. The previous data sources have indicated that the most significant factors which should be considered in a correlation for pressure drop of a gas-solid suspension are loading ratio η , gas Reynolds number Re_g , and particle diameter D_p . The application of the drag coefficient model not only appears difficult since V_p is not a readily available quantity but leads to incorrect results as illustrated by the work of Peskin and Dwyer; and Mehta, Smith, and Comings. Therefore, the subsequent analysis will be directed entirely towards the equivalent friction factor model in order to obtain a working correlation for f'_s/f_g , which then can be used to predict suspension pressure drops.

Equivalent friction factor based on eddy viscosity model. - In the eddy viscosity model proposed by Julian and Dukler (ref. 32), the value of the friction factor f'_s depends directly on the value of K , the modified von Kármán constant that appears in their expression for the eddy viscosity. On the basis of the experimental data of six independent investigations of gas-solid suspension pressure drop, Julian and Dukler concluded that K is a function of loading ratio η only (see eqs. (61) and (62)) and is independent of gas Reynolds number, particle diameter, and particle density. Based on the value of K given by equation (61), the dependence of f'_s on gas Reynolds number and loading ratio was obtained by Julian (ref. 32) and is plotted in figure 17. The plot shows that f'_s increases with solid loading ratio and decreases exponentially with increasing gas Reynolds number at constant η . The slope of the lines of constant η is approximately equal to -0.2 , which indicates that the effect of gas Reynolds number on the suspension flow is approximately the same as it is for pure gas flow (eq. (45)). Thus, for the range of conditions covered, f'_s/f_g is essentially independent of Re_g .

A cross plot of figure 17 giving f'_s as a function of $1 + \eta$ with Re_g as a parameter is presented in figure 18. For simplicity, these curves can be fitted approximately by

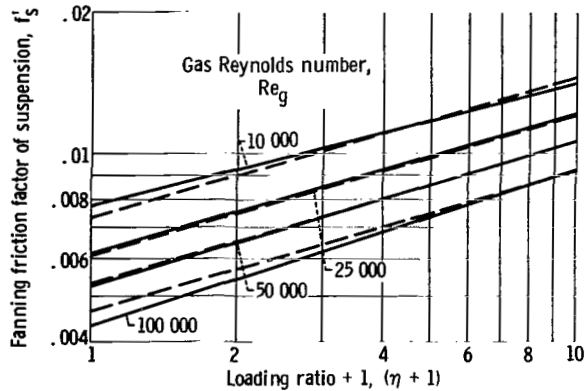


Figure 18. - Fanning friction factor of suspension as function of loading ratio plus one ($\eta + 1$) as predicted by reference 32. Dashed lines are plots of equation (69a).

the equation

$$f'_s = 0.046 \text{Re}_g^{-0.2} (1 + \eta)^{0.3} \quad (69a)$$

denoted by the dashed lines in figure 18.

Thus, a very simple approximation for the Julian and Dukler correlation can be obtained in terms of f'_s/f_g :

$$\frac{f'_s}{f_g} = (1 + \eta)^{0.3} \quad (69b)$$

Equivalent friction factor by use of Reynolds analogy. - The use of the Reynolds analogy in conjunction with the correlations of the heat-transfer coefficient represented by equations (44) and (43) yields four different friction factor correlations. Applying the Reynolds analogy separately to the particles and then superposing the two as in the manner of Gorbis (eq. (55)) yields the following two correlations:

$$\frac{f'_s}{f_g} = 1 + 4.0 \text{Re}_g^{-0.32} \eta \quad (70)$$

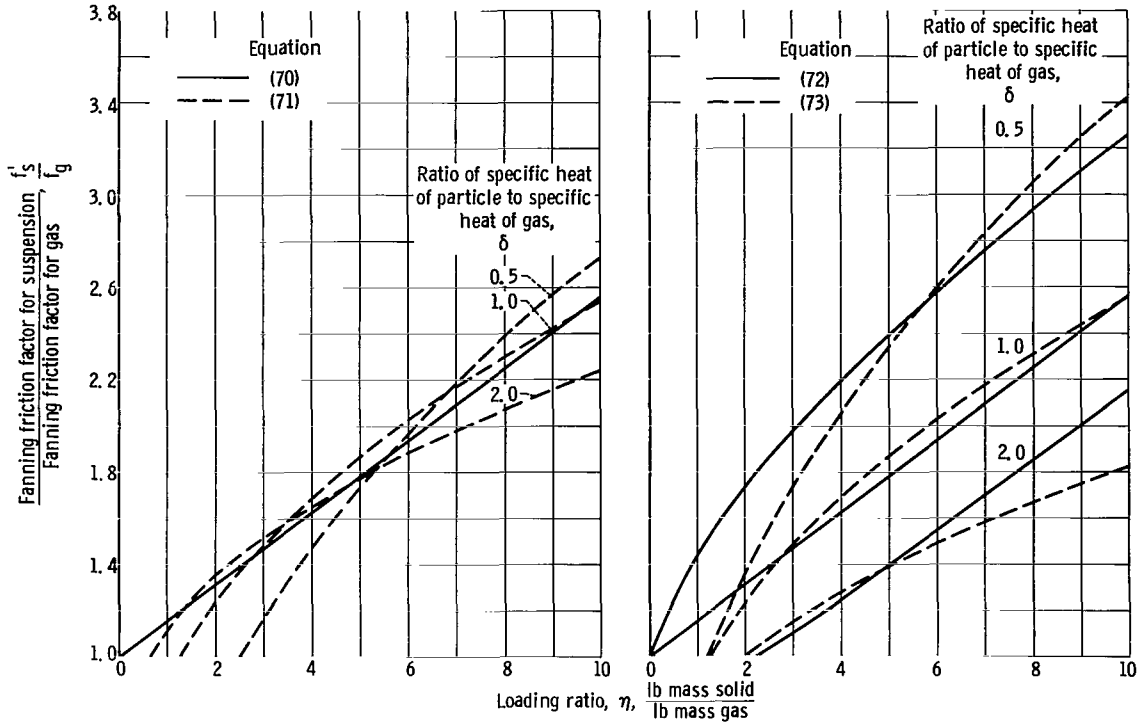
and

$$\frac{f'_s}{f_g} = 1 + \frac{1}{\delta} \left[7.6(\delta\eta)^{0.45} \text{Re}_g^{-0.21} - 1 \right] \quad (71)$$

Equation (70) is based on equation (44) for h_s/h_g , whereas equation (71) is based on equation (43) for h_s/h_g . In a similar manner, when the Reynolds analogy is applied directly to the suspension as given by equation (57), the correlations obtained from equations (44) and (43) are, respectively,

$$\frac{f'_s}{f_g} = \frac{\left(1 + 4.0 \text{Re}_g^{-0.32} \delta\eta \right) (1 + \eta)}{1 + \delta\eta} \quad (72)$$

and



(a) Superposition model.

(b) Suspension model.

Figure 19. - Comparison of Reynolds analogy correlations. Reynolds number, 25 000.

$$\frac{f'_s}{f_g} = \frac{7.6(\delta\eta)^{0.45} \text{Re}_g^{-0.21}(1 + \eta)}{1 + \delta\eta} \quad (73)$$

The four correlations obtained (eqs. (70), (71), (72), and (73)) are plotted as a function of η with δ as a parameter in figure 19 for a gas Reynolds number of 25 000. Figure 19(a) shows the correlations for the superposition model. With the superposition model and the heat-transfer correlation that leads to equation (70), the ratio of the equivalent friction factor of the suspension to the friction factor of the gas is independent of the specific heat ratio δ . Furthermore, when the heat-transfer correlation associated with equation (71) is used, the dependence of the equivalent friction factor ratio on δ is not large, especially for loading ratios between 4 and 10.

Figure 19(b) shows that the suspension model yields a considerable dependence of the equivalent friction factor ratio on the specific heat ratio. Use of either heat-transfer correlation gives about the same results. It should be pointed out that f'_s/f_g for equation (72) with $\delta = 2$ drops below unity for values of $\eta < 2$ before rising again to unity at $\eta = 0$.

A comparison of figures 19(a) and (b) shows that the two methods of applying the Reynolds analogy yield exactly the same results when $\delta = 1$; that is, equation (72)

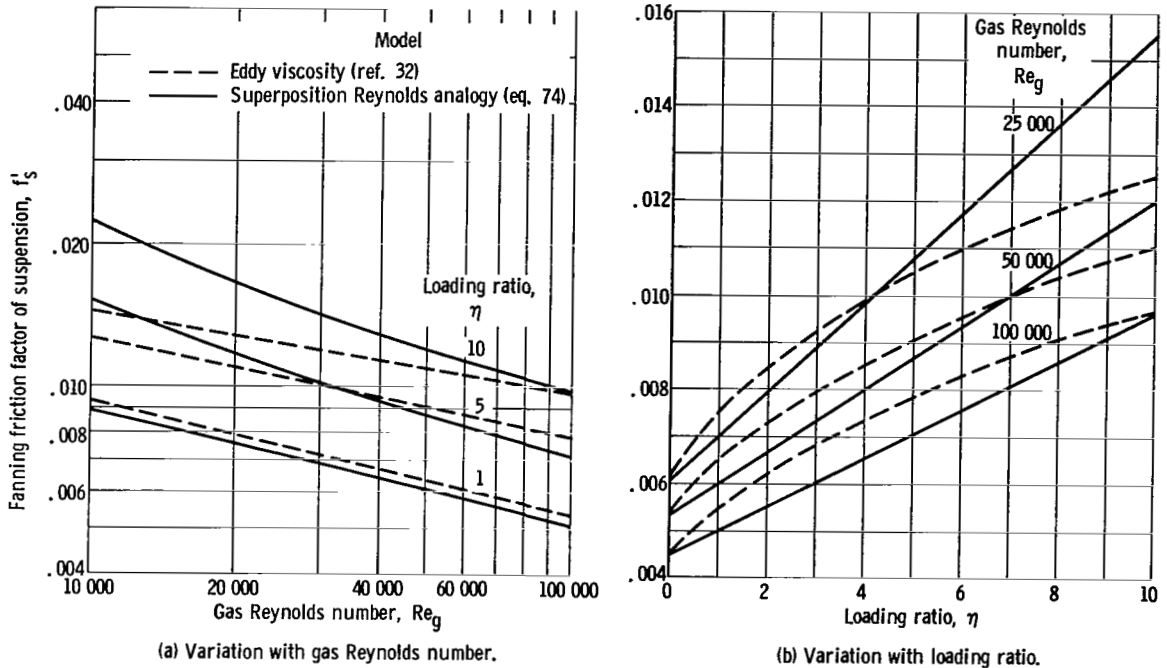


Figure 20. - Comparison of superposition Reynolds analogy with eddy viscosity model.

reduces to equation (70), and equation (73) reduces to equation (71).

Of the four possible correlations for f'_s/f_g , equation (70) is clearly the simplest, since it does not show a dependence on δ . It does not seem probable that the specific heats of the particles and the gas should affect pressure drop; in fact, specific heats have not been considered as a factor in any of the pressure drop literature. Therefore, until a definite effect of δ on pressure drop is established, it seems reasonable to consider only equation (70) to represent the Reynolds analogy. Equation (70) is also in the form of the original Gasterstadt equation (eq. (32)), which has been used for correlating pressure drop data by a number of investigators (refs. 42, 43, and 44) and which provides a ratio of unity at $\eta = 0$.

When equation (70) is multiplied by f_g (eq. (45)),

$$f'_s = 0.046 Re_g^{-0.2} + 0.184 Re_g^{-0.52} \eta \quad (74)$$

Figures 20(a) and (b) compare f'_s (as calculated by eq. (74)) to the curves obtained by Julian and Dukler (fig. 17). As can be seen from figure 20(a), the friction factor as predicted by the Reynolds analogy correlation shows a greater dependence on Re_g as η is increased than that found by Julian and Dukler.

At very low values for the loading ratios the first term on the right-hand side of equation (74) predominates, and f'_s is proportional to $Re_g^{-0.2}$. At very high values for the loading ratios the second term predominates, and f'_s is proportional to $Re_g^{-0.52}$.

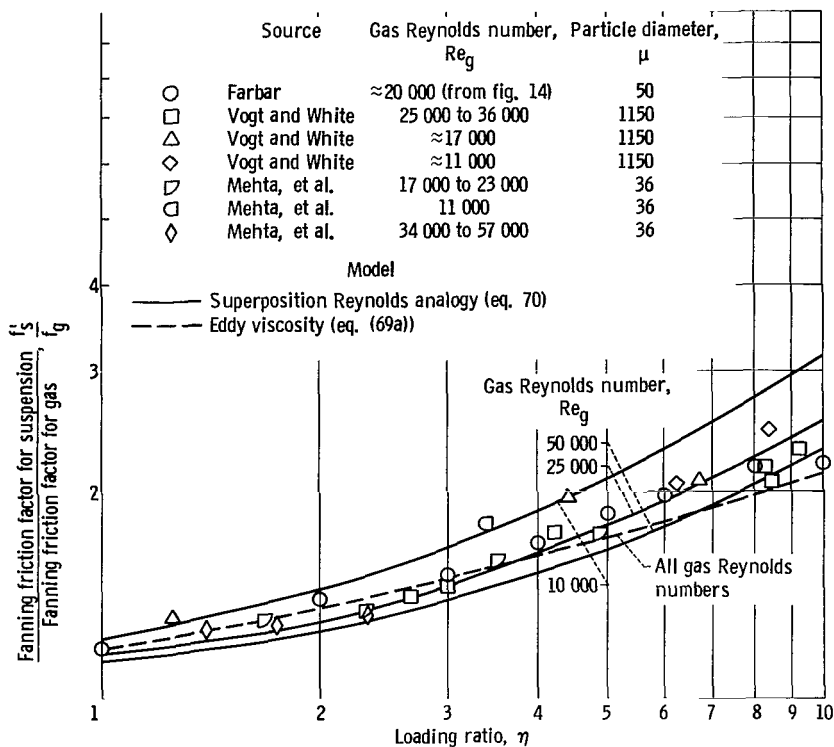


Figure 21. - Ratio of Fanning friction factor of suspension to friction factor of gas as function of loading ratio for various correlations and data sources.

Therefore, the Re_g dependence of f'_s varies between the -0.2 and -0.52 power of Re_g . Julian and Dukler found the dependence to remain at approximately the -0.2 power, as in the case of a pure gas. Nevertheless, the agreement between the eddy viscosity model and the Reynolds analogy is quite close at $Re_g > 25\ 000$.

It should be noted that most of the data upon which Julian and Dukler's correlation is based utilized gas Reynolds numbers ranging from approximately 30 000 to 100 000. The only data where lower Reynolds numbers were employed were the data of Depew and that of Hariu and Molstad. The data of Depew ($Re = 13\ 500$ to $27\ 400$) yield consistently higher results for f'_s than those predicted by Julian and Dukler. The data of Hariu and Molstad ($Re = 3700$ to $11\ 000$) corrected for acceleration effects by Julian, however, appear to be in agreement with the correlation.

Comparison of models with experimental data. - Figure 21 is a plot of f'_s/f_g against η as predicted by the Reynolds analogy (eq. (70)) with gas Reynolds number as a parameter. Julian and Dukler's eddy viscosity model appears as a single (dashed) curve independent of gas Reynolds number. The data of Mitlin; Hinkle; Clark, Charles, Richardson and Newitt; Depew; Hariu and Molstad; and Helander are adequately represented by this curve. The data of Mehta, Smith, and Comings ($36\text{-}\mu$ particles), Vogt and White's clover data, and points from Farbar's curve (see fig. 16) are also presented in the figure.

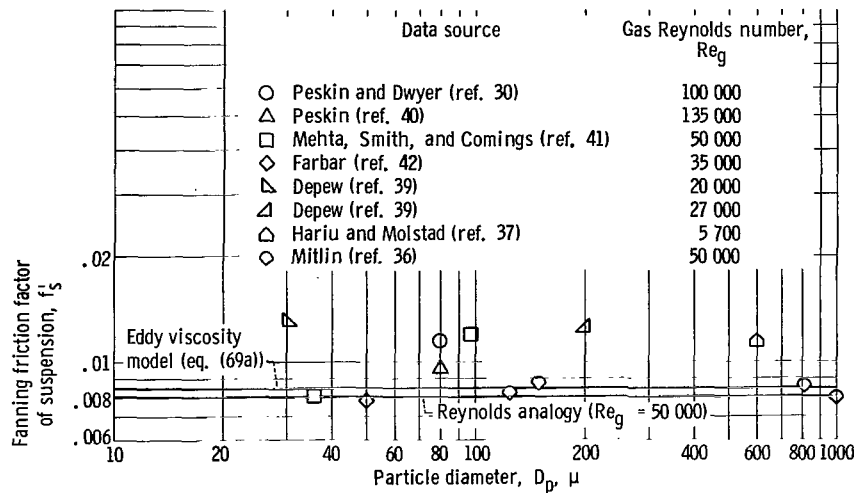


Figure 22. - Fanning friction factor of suspension as function of particle diameter. Loading ratio, $3 \leq \eta \leq 4$.

The agreement of these data with both the Reynolds analogy and the eddy viscosity model curve is very close, although a Reynolds number effect similar to that predicted by the Reynolds analogy seems to be discernible; that is, the data points at low gas Reynolds numbers are somewhat higher than those at high gas Reynolds numbers. These results are also in agreement with the correlation presented by Dogin and Lebedev (see eq. (67b)), where a similar type of gas velocity dependence is predicted.

At values of η between 4 and 10, figure 21 shows that the friction factor f'_s/f_g curves may be fitted by straight lines of slope of the order of 0.45 as was found for the heat-transfer coefficient correlation (eq. (43)). The data of Peskin; Mehta, Smith, and Comings; and Farbar also show approximately this same η dependence on the friction factor (see figs. 14 to 16), which is a good indication of the validity of the analogy.

Peskin's data; and Mehta, Smith, and Comings' 97-micron particle data have not been plotted in figure 21 since the absolute magnitude of their data is much higher than predicted by the eddy viscosity model or the Reynolds analogy and is in disagreement with most of the other data previously discussed.

Effect of particle diameter. - Since the heat-transfer correlations utilized (eqs. (43) and (44)) showed essentially no particle diameter dependence, the friction factor correlations naturally show no particle diameter effect. This fact is in agreement with the findings of Julian and Dukler, who could discover no apparent particle diameter effect on f'_s for the data that they investigated, which included a particle diameter range from 25 to 6000 microns. Figure 22 is a plot of f'_s against particle diameter obtained from the experimental data for loading ratios between 3 and 4. Although the data do not fall on a single horizontal line (which would indicate no particle diameter effect), no other obvious particle diameter effect is evident. Therefore, the conclusion that particle diameter has no effect as predicted by both the eddy viscosity model and the Reynolds

analogy must be accepted until further data become available.

Final correlations. - As a result of the preceding analysis, it would appear that for the range of variables covered in the literature either the following correlation obtained using the Reynolds analogy

$$\frac{f'_s}{f_g} = 1 + 4.0 \operatorname{Re}_g^{-0.32} \eta \quad (70)$$

or the eddy viscosity model as proposed by Julian and Dukler, which can be expressed approximately as

$$\frac{f'_s}{f_g} = (1 + \eta)^{0.3} \quad (69b)$$

yields values of f'_s/f_g , which are in agreement with most of the experimental data. Both correlations are therefore recommended for predicting pressure drops associated with the fully developed turbulent flow of gas-solid suspensions in smooth tubes.

APPLICATION OF RESULTS

The correlations obtained as a result of this analysis should be applied in flow system calculations with heat transfer only after first examining the various limitations implicit in their development. Aside from the restrictions with respect to gas Reynolds number, particle diameter, and loading ratio previously indicated there are other less obvious restraints and implications. These factors arise from the fact that the experimental data from which the correlations were developed were obtained for certain combinations of gases and particles at certain test conditions; that is, fixed pressures, temperatures, heat fluxes, velocities, and pipe diameters.

For the heat-transfer coefficient, the test data in the survey covered pressures from 0 to 130 pounds per square inch gage, temperatures from 75^o to 1100^o F, velocities from about 1 to 200 feet per second, and pipe diameters from 0.3 to 4 inches. In practically all cases, heat was added to the suspension flow. For the friction factor, all tests were run at essentially adiabatic conditions at low temperatures (~70^o F). The range of pressures, velocities, and pipe inside diameters for this factor were, respectively, 0 to 30 pounds per square inch gage, 10 to 150 feet per second, and 0.25 to 5 inches. For both the heat-transfer and friction factor tests, the flow could be considered as fully developed turbulent flow.

In applying the correlations obtained herein to calculations for any other system the following procedure is recommended. The following equation may be used for the suspension heat-transfer coefficient

$$h_s = \left(\frac{h_s}{h_g} \right)_{\text{corr}} h_g \quad (75)$$

where $(h_s/h_g)_{\text{corr}}$ is obtained from the appropriate correlation presented herein. Thus, all that need be done is to compute $(h_s/h_g)_{\text{corr}}$ and h_g , both evaluated at the temperature, pressure, velocity, and pipe diameter associated with the gas in the suspension flow. It should be pointed out, however, that in various application systems all these variables may not be independent. For example, in a Brayton power cycle, the local pressure, temperature, and volumetric flow rate are interrelated through the cycle input parameters. Furthermore, these local state values may in turn also be functions of the suspension loading ratio.

In a manner similar to that used for the suspension heat-transfer coefficient, the suspension effective friction factor can be found from

$$f'_s = \left(\frac{f'_s}{f_g} \right)_{\text{corr}} f_g \quad (76)$$

where both f_g and $(f'_s/f_g)_{\text{corr}}$ are to be evaluated in the same manner as outlined for $(h_s/h_g)_{\text{corr}}$ and h_g . It is apparent, therefore, that in using the preceding procedure, correlations of the form of equations (44) and (70) are preferred as they conveniently reduce to unity when $\eta = 0$.

Strictly speaking, in equations (75) and (76), both h_g and f_g refer to the values of h_s and f'_s for $\eta = 0$; however, for practical purposes, h_g and f_g can be evaluated from appropriate, available pure gas correlations.

The question also exists of the applicability of the selected correlations for $(h_s/h_g)_{\text{corr}}$ and $(f'_s/f_g)_{\text{corr}}$ to gases, particles, state conditions, and heat-transfer methods different from those covered in the referenced experimental data. However, in view of the approximate nature of the correlation and the large scatter in the referenced data, such questions may not be serious for preliminary calculations.

In order to increase the correlation precision, further work over a wide range of gases, particles, heat-transfer methods, heat fluxes, temperatures, pressures, velocities, and pipe diameters is desirable. This experimental work should include pure gas ($\eta = 0$) data with the same apparatus because these data may not be in exact agreement with the established pure gas correlations.

SUMMARY OF RESULTS

The published literature data concerning the heat-transfer and pressure drop associated with the flow of dilute gas-solid suspensions were analyzed. Although the available data were insufficient and somewhat inconsistent for precise correlation, approximate relations for preliminary use in predicting suspension heat-transfer coefficients and friction factors were developed. Two possible correlations were developed for the heat-transfer coefficient ratio. From these correlations and the available data, it was found that

1. The ratio of the heat-transfer coefficient of a suspension to the heat-transfer coefficient of an equal volumetric rate of flow of gas at the same pressure and temperature increases with loading ratio (lb solid/lb gas).
2. The heat-transfer coefficient ratio increases as the ratio of particle specific heat to pure gas specific heat is increased.
3. The heat-transfer coefficient ratio decreases as the gas Reynolds number is increased.
4. The particle diameter has little effect on the ratio of heat-transfer coefficients for the range of particle sizes between 30 and 150 microns.

Application of the Reynolds analogy to these heat-transfer correlations yielded a relation for the ratio of equivalent friction factor of a suspension to the equivalent friction factor of a gas. This relation indicates the following:

1. The friction factor ratio increases as the loading ratio is increased.
2. The friction factor ratio decreases as the gas Reynolds number is increased.
3. The particle diameter and specific heat appeared to have little or no effect on the friction factor.

The results of experimental data available in the literature as well as an analytical study of the equivalent friction factor using an eddy viscosity model for the suspension compare quite favorably with the developed friction factor correlation especially at low loading ratios ($\eta < 5$). However, it was evident from the correlations of both the heat-transfer coefficient and the equivalent friction factor data that additional experimental investigations may be required to obtain more precise variations for specific particles and variable ranges of interest.

Lewis Research Center,
National Aeronautics and Space Administration,
Cleveland, Ohio, April 12, 1966.

APPENDIX - SYMBOLS

a	constant (eq. (35))	f'_p	particle Fanning friction factor based on velocity of particle and particle density in mixture
a'	experimentally determined constant (eq. (63))		
B	constant (eq. (68)) depending upon solid-gas system	f_s	Fanning friction factor for suspension based on velocity and density of suspension
b	constant (eq. (36))		
C	constant (eq. (67b)) depending upon gas-solid system	f'_s	Fanning friction factor based on velocity of suspension and density of gas
C_D	standard drag coefficient for spherical particles	g	acceleration of gravity, ft/sec ²
$(C_p)_g$	specific heat of gas, Btu/(lb)(°F)	g_c	gravitational constant, (lb mass)(ft)/(lb force)(sec ²)
$(C_p)_p$	specific heat of particles, Btu/(lb)(°F)	h_g	convective heat-transfer coefficient for pure gas, Btu/(hr)(ft ²)(°F)
$(C_p)_s$	specific heat of suspension, Btu/(lb)(°F)	h_p	convective heat-transfer coefficient, Btu/(hr)(ft ²)(°F) (eq. (27))
D	tube inside diameter, ft	h_s	convective heat-transfer coefficient for suspension, Btu/(hr)(ft ²)(°F)
D_p	diameter of particle, μ or ft	K	von Kármán constant for a pure gas and a function of η for a suspension
F	complicated function of gas Reynolds number and other parameters in Gasterstadt equation (eq. (32))	k	experimentally determined constant (eq. (60))
F_D	drag force, lb	k_g	thermal conductivity of pure gas, Btu/(hr)(ft)(°F)
Fr_g	Froude number for gas	k_p	thermal conductivity of particle, Btu/(hr)(ft)(°F)
f_g	Fanning friction factor for pure gas	k_s	thermal conductivity of suspension, Btu/(hr)(ft)(°F)
f_m	mixture Fanning friction factor (eq. (63))		
f_p	particle Fanning friction factor based on velocity of particle and density of gas		

k_1, k_2, k_3, k_4	constants when all parameters except η are fixed	T_m	mean temperature of wall and suspension, $^{\circ}\text{R}$
k'_1, k'_2, k'_4	constants when all parameters except δ and η are fixed	T_p	temperature of particle, $^{\circ}\text{F}$
L	length of tube, length of calming plus test sections, ft	T_s	bulk temperature of suspension, $^{\circ}\text{R}$
l	exponent in equation (68) and function of dimensionless group, $\text{Re}_p(C_d)^{1/2}$	V_g	gas velocity, ft/sec
m	experimentally determined constant (eq. (60))	V_p	velocity of particle, ft/sec
Nu_g	Nusselt number of pure gas	V_{ps}	terminal settling velocity of particle, ft/sec
Nu_s	Nusselt number of suspension	V_s	velocity of suspension, ft/sec
n	number of particles per cubic foot of mixture, particles/ft ³	W_g	mass flow rate of pure gas, lb/sec
ΔP_g	pressure drop caused by gas flow, lb force/ft ²	W_p	mass flow rate of solids, lb/sec
ΔP_p	additional pressure drop caused by adding particles to gas stream, lb force/ft ²	y	radial distance from tube wall, ft
ΔP_s	pressure drop caused by suspension flow, lb force/ft ²	y_m^+	dimensionless distance from tube wall evaluated at center of tube
Pr_g	Prandtl number of pure gas	α_g	sonic velocity of pure gas, ft/sec
Pr_s	Prandtl number of suspension	α_s	sonic velocity of suspension, ft/sec
Re_g	Reynolds number of pure gas	β	$\frac{[1 + (k_p/k_g)]}{[1 - (k_p/k_g)]}$
Re_p	particle Reynolds number	γ_g	isentropic specific heat ratio for pure gas
Re_s	Reynolds number of suspension	γ_s	isentropic specific heat ratio for suspension
T_g	temperature of gas, $^{\circ}\text{F}$	δ	ratio of specific heat of particle to specific heat of gas
		ϵ	fractional solid volume, ft ³ solid/ft ³ suspension

ϵ'	eddy viscosity, ft^2/hr	ρ_p	particle density, lb/ft^3 solid
η	loading ratio, lb mass solid/lb mass gas	ρ'_p	density of solid, lb solid/ ft^3 suspension
μ_g	viscosity of pure gas, lb/(ft)(hr)	ρ_s	bulk density of suspension, lb/ ft^3 suspension
μ_s	viscosity of suspension, lb/(ft)(hr)	φ	constant, $(y_m^+ - 60)/22$
ρ_g	density of pure gas, lb/ ft^3 gas	ψ	factor characteristic of loading ratio (eq. (7a))

REFERENCES

1. Glassman, Arthur J.; and Stewart, Warner L.: Thermodynamic Characteristics of Brayton Cycles for Space Power. *J. Spacecraft Rockets*, vol. 1, no. 1, Jan. - Feb. 1964, pp. 25-31.
2. Stewart, Warner L.; Glassman, Arthur J.; and Krebs, Richard P.: The Brayton Cycle for Space Power. Paper No. 741A, SAE, 1963.
3. Glassman, A. J.; Krebs, R. P.; and Fox, T. A.: Brayton Cycle Nuclear Space System and Their Heat-Transfer Components. Paper No. 57, A. I. Ch. E., 1963.
4. Farbar, Leonard; and Morley, Morgan J.: Heat Transfer to Flowing Gas-Solids Mixtures in a Circular Tube. *Ind. Eng. Chem.*, vol. 49, no. 7, July 1957, pp. 1143-1150.
5. Danziger, W. J.: Heat Transfer to Fluidized Gas-Solids Mixtures in Vertical Transport. *Ind. Eng. Chem. (Process Design and Dev.)*, vol. 2, no. 4, Oct. 1963, pp. 269-276.
6. Gorbis, Z. R.; and Bakhtiozin, R. A.: Investigation of Convection Heat Transfer to a Gas-Graphite Suspension Under Conditions of Internal Flow in Vertical Channels. *Soviet J. Atomic Energy*, vol. 12, no. 5, Nov. 1962, pp. 402-409.
7. Gorring, Robert L.; and Churchill, Stuart W.: Thermal Conductivity of Heterogeneous Materials. *Chem. Eng. Prog.*, vol. 57, no. 7, July 1961, pp. 53-59.
8. Sproull, W. T.: Viscosity of Dusty Gases. *Nature*, vol. 190, no. 4780, June 10, 1961, pp. 976-978.
9. Happel, John: Viscosity of Suspensions of Uniform Spheres. *J. Appl. Phys.* vol. 28, no. 11, Nov. 1957, pp. 1288-1292.
10. Einstein, A.: New Determination of Molecular Dimensions. *Ann. Physik*, vol. 19, no. 2, Feb. 8, 1906, pp. 289-306.
11. Kliegel, J. R.; and Nickerson, G. R.: Flow of Gas-Particle Mixtures in Axially Symmetric Nozzles. Rept. No. TR-59-0000-00746, Space Technology Labs., 1959.
12. Soo, S. L.: Gas Dynamic Processes Involving Suspended Solids. *A. I. Ch. E., J.*, vol. 7, no. 3, Sept. 1961, pp. 384-391.
13. Kliegel, James R.: Gas Particle Nozzle Flows. Ninth International Symposium on Combustion, W. G. Berl, ed., Academic Press, 1963, pp. 811-826.

14. Foust, Alan S.; Wenzel, Leonard A.; Clump, Curtis W.; Maus, Louis; and Andersen, L. Bryce: Principles of Unit Operations. John Wiley & Sons, Inc., 1960.
15. Farbar, Leonard; and Depew, Creighton A.: Heat Transfer Effects to Gas-Solids Mixtures Using Solid Spherical Particles of Uniform Size. Ind. Eng. Chem. Fundamentals, vol. 2, no. 2, May 1963, pp. 130-135.
16. Anon.: Gas-Suspension Coolant Project. Rept. No. BAW-1159, The Babcock and Wilcox Co., Aug. 1959.
17. Anon.: Gas Suspension Task II. Rept. No. BAW-1181, The Babcock and Wilcox Co., Nov. 1959.
18. Schluderberg, Donald C.; Whitelaw, R. L.; and Carlson, Robert W.: Gaseous Suspensions - A New Reactor Coolant. Nucleonics, vol. 19, no. 8, Aug. 1961, pp. 67-68; 70; 72; 74; 76.
19. Wachtell, G. P.; Waggener, J. P.; and Steigelmann, W. H.: Evaluation of Gas-Graphite Suspensions as Nuclear Reactor Coolants. Rept. No. NYO-9672, AEC, Aug. 1961.
20. Gasterstadt, J.: Die Experimentelle Untersuchung des Pneumatischen Fördervorgangs. Forsch. - Arb. Ing. - Wes., No. 265, 1924, p. 1.
21. Zenz, Frederick A.; and Othmer, D. F.: Fluidization and Fluid-Particle Systems. Reinhold Publishing Corp., 1960.
22. Tien, C. L.: Heat Transfer by a Turbulently Flowing Fluid-Solids Mixture in a Pipe. J. Heat Transfer, vol. 83, no. 2, May 1961, pp. 183-188.
23. Tien, C. L.; and Quan, V.: Local Heat Transfer Characteristics of Air-Glass and Air-Lead Mixtures in Turbulent Pipe Flow. Paper No. 62-HT-15, ASME, Aug. 1962.
24. Mickley, Harold S.; and Trilling, Charles A.: Heat Transfer Characteristics of Fluidized Beds. Ind. Eng. Chem., vol. 41, no. 6, June 1949, pp. 1135-1147.
25. List, H. L.: Heat Transfer to Flowing Gas-Solids Mixtures. Ph.D. Thesis, Polytech. Inst. of Brooklyn, 1958.
26. Anon: High-Temperature Energy Systems. Quarterly Progr. Rep., Bureau of Mines, Morgantown, Aug. 1-Oct. 31, 1964. (AEC Rep. No. TID-21596.)
27. Soo, S. L.: Fully Developed Turbulent Pipe Flow of a Gas-Solid Suspension. Ind. Eng. Chem. Fundamentals, vol. 1, no. 1, Feb. 1962, pp. 33-37.

28. Soo, S. L.; Trezek, G. J.; Dimick, R. C.; and Hohnstreiter, G. F.: Concentration and Mass Flow Distributions in a Gas-Solid Suspension. *Ind. Eng. Chem. Fundamentals*, vol. 3, no. 2, May 1964, pp. 98-106.
29. Korn, Arthur H.: How Solids Flow in Pneumatic Handling Systems. *Chem. Eng.*, vol. 57, no. 3, Mar. 1950, pp. 108-111.
30. Peskin, R. L.; and Dwyer, H. A.: A Study of the Mean-Flow Characteristics of Gas-Solid Suspensions. Rept. No. NYO-2930-1 (101-ME-F), AEC, Feb. 1964.
31. Hinkle, B. L.: Acceleration of Particles and Pressure Drops Encountered in Pneumatic Conveying. Ph.D. Thesis, Georgia Inst. Tech., 1963.
32. Julian, F. M.; and Dukler, A. E.: An Eddy Viscosity Model for Friction in Gas-Solids Flow. A.I.Ch.E. Paper presented at the Symposium on Selected Papers - Part III, Fifty-Sixth National Meeting, May 16-19, 1965.
33. Gill, William N.; and Scher, Marvin: A Modification of the Momentum Transport Hypothesis. *A.I.Ch.E., J.*, vol. 7, no. 1, Mar. 1961, pp. 61-63.
34. Deissler, Robert G.: Analytical and Experimental Investigation of Adiabatic Turbulent Flow in Smooth Tubes. NACA TN 2138, 1950.
35. Helander, R. E.: The Flow Characteristics of Air-Solids Mixtures. Ph.D. Thesis, Northwestern Univ., 1956.
36. Mitlin, L.: A Study of Pneumatic Conveying with Special Reference to Particle Velocity and Pressure Drop During Transport. Ph.D. Thesis, Univ. of London, 1954.
37. Hariu, O. H.; and Molstad, M. C.: Pressure Drop in Vertical Tubes in Transport of Solids by Gases. *Ind. Eng. Chem.*, vol. 41, no. 6, June 1949, pp. 1148-1160.
38. Clark, R. H.; Charles, D. E.; Richardson, J. F.; and Newitt, D. M.: Pneumatic Conveying. Pt. I. The Pressure Drop During Horizontal Conveyance. *Trans. Inst. Chem. Eng.*, vol. 30, no. 4, 1952, pp. 209-224; vol. 31, no. 1, 1953, pp. 94-95.
39. Depew, C. A.: Heat Transfer to Flowing Gas-Solids Mixtures in a Vertical Circular Duct. Ph.D. Thesis, Univ. of Calif., 1960.
40. Peskin, R. L.: Basic Studies in Gas-Solid Suspension. Quarterly Rep. Nos. 63-1 and 64-1, Rutgers Univ., 1963. (Contract No. AT(30-1)2930).
41. Mehta, N. C.; Smith, J. M.; and Comings, E. W.: Pressure Drop in Air-Solid Flow Systems. *Ind. Eng. Chem.*, vol. 49, no. 6, June 1957, pp. 986-992.

42. Farbar, Leonard: Flow Characteristics of Solids-Gas Mixtures in a Horizontal and Vertical Circular Conduit. *Ind. Eng. Chem.*, vol. 41, no. 6, June 1949, pp. 1184-1191.
43. Dogin, M. E.; and Lebedev, V. P.: Dependence of the Resistance in Pneumatic-Conveying Pipelines on the Fundamental Parameter of Two-Phase Flow. *Ind. Chem. Eng.*, vol. 2, no. 1, Jan. 1962, pp. 64-67.
44. Vogt, E. G.; and White, R. R.: Friction in the Flow of Suspensions - Granular Solids in Gaseous Through Pipe. *Ind. Eng. Chem.*, vol. 40, no. 9, Sept. 1948, pp. 1731-1738.
45. Belden, D. H.; and Kassel, Louis S.: Pressure Drops Encountered in Conveying Particles of Large Diameter in Vertical Transport Lines. *Ind. Eng. Chem.*, vol. 41, no. 6, June 1949, pp. 1174-1178.
46. Julian, F. M.: A Study of Pressure Drop in Gas-Solid Flow. M.S. Thesis, Univ. of Houston. May 1964.

"The aeronautical and space activities of the United States shall be conducted so as to contribute . . . to the expansion of human knowledge of phenomena in the atmosphere and space. The Administration shall provide for the widest practicable and appropriate dissemination of information concerning its activities and the results thereof."

—NATIONAL AERONAUTICS AND SPACE ACT OF 1958

NASA SCIENTIFIC AND TECHNICAL PUBLICATIONS

TECHNICAL REPORTS: Scientific and technical information considered important, complete, and a lasting contribution to existing knowledge.

TECHNICAL NOTES: Information less broad in scope but nevertheless of importance as a contribution to existing knowledge.

TECHNICAL MEMORANDUMS: Information receiving limited distribution because of preliminary data, security classification, or other reasons.

CONTRACTOR REPORTS: Technical information generated in connection with a NASA contract or grant and released under NASA auspices.

TECHNICAL TRANSLATIONS: Information published in a foreign language considered to merit NASA distribution in English.

TECHNICAL REPRINTS: Information derived from NASA activities and initially published in the form of journal articles.

SPECIAL PUBLICATIONS: Information derived from or of value to NASA activities but not necessarily reporting the results of individual NASA-programmed scientific efforts. Publications include conference proceedings, monographs, data compilations, handbooks, sourcebooks, and special bibliographies.

Details on the availability of these publications may be obtained from:

SCIENTIFIC AND TECHNICAL INFORMATION DIVISION
NATIONAL AERONAUTICS AND SPACE ADMINISTRATION

Washington, D.C. 20546